

Report No. 1100539.401
Revision 1
Project No. 1100539
July 2011

This document is a non-proprietary version of SIA Report No. 1100539.401. EPRI/BWRVIP proprietary information removed from the SIA report is indicated by braces "{ }" or clouds.

**Nine Mile Point Unit 1
Steam Dryer Support Bracket Flaw Evaluation**

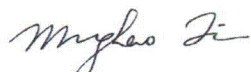
Prepared for:

Constellation Energy Nuclear Group
Lycoming, NY
PO Number 7722655, Rev. 1

Prepared by:

Structural Integrity Associates, Inc.
San Jose, California

Prepared by:



Minghao Qin

Date: 7/8/11

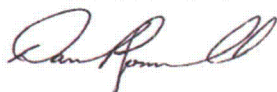
Reviewed by:



Matthew Walter
Hal Gustin, P.E.

Date: 7/8/11

Approved by:



Daniel Sommerville, P.E.

Date: 7/8/11

REVISION CONTROL SHEET

Document Number: 1100539.401

Title: Nine Mile Point Unit 1 Steam Dryer Support Bracket Flaw Evaluation

Client: Constellation Energy Nuclear Group

SI Project Number: 1100539

Quality Program: Nuclear Commercial

Pages	Revision	Date	Comments
1-41 A-1 – A-6	0	4/14/2011	Initial Issue
1, 14-16, 18, 20, 23, 28-30 A-1 – A-6	1	7/8/2011	Added allowable flaw sizes for two crack cases using both limit load and LEFM. Added two additional modeling assumptions which were present in Rev. 0 analysis but were not clearly documented. Added plastic zone size correction for the LEFM evaluation.

Table of Contents

<u>Section</u>	<u>Page</u>
1.0 INTRODUCTION.....	1
2.0 PURPOSE.....	2
3.0 DESIGN INPUTS	2
4.0 METHODOLOGY	4
4.1 Loads.....	5
4.2 Flaw Characterization	9
4.3 NDE Uncertainty	9
4.4 Crack Growth.....	9
4.5 Failure Mechanisms	10
4.6 Analysis Methods.....	10
4.6.1 <i>Limit Analysis</i>	10
4.6.2 <i>Linear Elastic Fracture Mechanics Analysis</i>	13
4.6.3 <i>Functional Evaluation</i>	14
4.6.4 <i>Qualitative Assessment of Radially Oriented Indication in 1-587A</i>	15
4.6.5 <i>Method for Determining Allowable Flaw Size</i>	15
5.0 ASSUMPTIONS.....	17
6.0 CONSERVATISMS.....	19
7.0 ANALYSIS	20
7.1 Flaw Characterization and Summary	21
7.2 Flaw Growth	21
7.3 Linear Elastic Fracture Mechanics Analysis.....	23
7.4 Limit Analysis.....	23
7.5 Functional Analysis	26
7.6 Qualitative Assessment of Radial Indication in 1-587A.....	27

7.7	Allowable Flaw Sizes	28
7.7.1	<i>Limit Load Allowable Flaw Sizes</i>	28
7.7.2	<i>LEFM Allowable Flaw Size</i>	29
7.7.3	<i>Summary of the Allowable Flaw Sizes</i>	30
8.0	CONCLUSIONS	30
9.0	REFERENCES	32
	APPENDIX A LEFM ANALYSIS	A-1

List of Tables

<u>Table</u>	<u>Page</u>
Table 1: Summary of Steam Dryer Support Bracket Loads.	8
Table 2: Summary of Load Cases Evaluated for Level A/B Limit Analysis.....	12
Table 3: Summary of LEFM Evaluation.	23

List of Figures

<u>Figure</u>	<u>Page</u>
Figure 1. Photographs of NMP1 Steam Dryer Support Bracket Configuration.	34
Figure 2. Schematic of Steam Dryer Support Bracket Configuration.	35
Figure 3. Schematic Illustrating Location of Applied Loads on Steam Dryer Support Bracket.	36
Figure 4. Overlay of Inspection Data.....	37
Figure 5. Initial Flaw Characterization (without NDE uncertainty).....	38
Figure 6. End of Evaluation Interval Flaws (with NDE uncertainty and growth).....	38
Figure 7. Crack Cases Selected for Flaw Evaluation.....	39
Figure 8. 2-D Edge Cracked Finite Width Plate LEFM Solution for In-Plane and Out of Plane Shear.	39
Figure 9. 2-D LEFM Solution Perpendicular Plates Subjected to Axial Force, Bending Moment, and Uniform Membrane Stress in Semi-Infinite Wall.....	40
Figure 10. FEM and Results of Plastic Collapse Benchmark.....	41
Figure 11. Steam Dryer Support Bracket FEM.	41
Figure 12. Finite Element Mesh for 0.2 inch Mesh Defined for Support Bracket.	42
Figure 13. Finite Element Mesh for 0.1 inch Mesh Defined for Support Bracket.	42
Figure 14. Loads and Boundary Conditions Applied to Support Bracket FEM.....	43
Figure 15. Von Mises Stress for EVT-1 Crack Case 1, 0.1 inch Mesh.	43
Figure 16. Von Mises Stress on the Crack Plane, EVT-1 Crack Case 1.	44
Figure 17. Hydrostatic Stress on the Crack Plane, EVT-1 Crack Case 1.	44
Figure 18. Maximum Principal Stress on the Crack Plane, EVT-1 Crack Case 1.....	44

Figure 19. Von Mises Strain on the Crack Plane, EVT-1 Crack Case 1.	45
Figure 20. Von Mises Stress (top left), Von Mises Strain (top right), Maximum Principal Stress (bottom left), and Hydrostatic Stress (bottom right) on the Crack Plane, Crack Case UT-1.	45
Figure 21. Von Mises Stress (top left), Von Mises Strain (top right), Maximum Principal Stress (bottom left), and Hydrostatic Stress (bottom right) on the Crack Plane, Crack Case EVT-2.....	46
Figure 22. Steam Dryer Hold-down Assembly Configuration.	47
Figure 23. Photograph of Steam Dryer Hold-down Assembly in Open Configuration (Not Installed on Support Bracket).....	47
Figure 24. End of Interval Allowable Flaw Sizes.....	48

1.0 INTRODUCTION

Reportable indications were identified in three of the four steam dryer support brackets at Nine Mile Point Unit 1 (NMP1) during the Spring 2011 Refueling Outage (RFO21) in-vessel visual inspections (IVVI) [1]. A supplementary ultrasonic (UT) examination of the dryer support brackets was also performed in RFO21 [2]. The support brackets were previously inspected in 2001 using a similar inspection technique without any reportable indications [2]. The three steam dryer support brackets with reportable indications are 1-587A, 1-587B, and 1-587C. Figure 1 is a compilation of photographs which show the configuration of the support brackets. Figure 2 is a schematic showing the nominal dimensions of the steam dryer support bracket configuration. The materials and component names used in this report are contained in this Figure for reference.

Cracking in steam dryer support brackets has been previously observed in other operating Boiling Water Reactors (BWRs) as documented in the Boiling Water Reactor Vessel and Internals Project (BWRVIP) Inspection and Evaluation Guideline written for vessel brackets and attachments (BWRVIP-48-A) [3]. BWRVIP-48-A [3] provides general guidance regarding performance of a flaw evaluation for the steam dryer support brackets. Constellation Energy Nuclear Group (CENG) has contracted with Structural Integrity Associates, Inc. (SI) to perform a flaw evaluation of the indications identified in the NMP1 steam dryer support brackets.

In this revision, the allowable flaw sizes, for two crack configurations, for the support brackets, considering both limit load and Linear Elastic Fracture Mechanics (LEFM) methods are calculated. The allowable flaw sizes are reported both including and excluding one cycle of Intergranular Stress Corrosion Cracking (IGSCC) and fatigue crack growth (FCG). The ASME III primary local membrane and local membrane plus bending stress intensity in the reactor pressure vessel (RPV) shell are checked to ensure the stress intensities remain within the ASME Code allowable stress criteria.

2.0 PURPOSE

The objective of the analysis documented in this report is to perform a flaw evaluation of the indications identified in the NMP1 steam dryer support brackets for an evaluation interval of one operating cycle to demonstrate that the structural margins contained in ASME B&PV Code Section XI are maintained throughout the evaluation interval, including consideration of flaw growth and continuing structural adequacy.

3.0 DESIGN INPUTS

The following design inputs are used in the analysis:

1. Operating cycle duration: 2 years [2]
2. Inspection Data: [1, 2, 10, 11]
3. Steam Dryer Support Bracket dimensions and materials: [4,5 Attachment 3]
4. Steam Dryer Support Bracket fabrication information: [5 Attachment 3]
5. Reactor Pressure Vessel (RPV) dimensions and materials: [6]
6. Steam Dryer dimensions: [4d]
7. ASME XI Code Year and Addenda: 2004 Ed., No Addenda [2]
8. Support Bracket Loads [2, 7, 8, 9]

The inspection data used for this evaluation are contained in the issued inspection reports as well as additional inspection photographs taken by the inspection personnel. All inspection data used for this evaluation are contained in the project files under the file 1100539.201, 1100539.204, and 1100539.210 [1, 2, 10, 11].

The inspection reports identify four indications in 1-587A. One indication is damage to the corner of the bracket at the top surface at the free edge of the bracket. This indication appears as though the corner of the bracket was damaged at some point; however, there are no crack like indications emanating from this damage which require evaluation. 1-587A also has two flaws on the bottom surface and lower portion of the left side of the bracket near the heat affected zone (HAZ) of the vessel attachment weld in the stainless steel base material. These flaws were

confirmed by UT. 1-587A also has a linear indication on the bottom surface of the bracket near the midpoint of the bracket width oriented parallel to the plane formed by the reactor pressure vessel (RPV) longitudinal axis and the radial direction of the RPV at the free surface. This indication was not confirmed by UT.

Bracket 1-587B has two linear indications on the top and right surfaces of the bracket near the HAZ of the vessel attachment weld in the stainless steel base material. The indication on the top surface of the bracket was confirmed by UT; the indication on the right surface of the bracket was not confirmed by UT because no scan was performed in this region. 1-587B also has a linear indication on the bottom surface of the bracket in the stainless steel base material adjacent to the vessel attachment weld HAZ. This indication was not detected by UT. The indication may be too shallow to detect using UT.

Bracket 1-587C has two indications on the top and right sides of the bracket in the stainless steel side of the vessel attachment weld in the HAZ. Both indications were confirmed by UT. Figure 4 summarizes the inspection results from both the EVT-1 and UT inspections on schematics of each bracket. Dimensions of each indication are provided in Figure 4.

The steam dryer support bracket dimensions are taken from the vessel drawing [4c], the fabrication drawing [4b], and the original stress analysis [7]. Assumptions are made where dimensional information is not available. These assumptions are discussed in Section 5 and supported by the available inspection photographs [1, 10, 11].

The steam dryer support bracket assembly materials are identified in References [4b, 5, 6] as:

- RPV Shell: SA-302, Grade B [6]
- Support Bracket: SA-240, Type 304 [4b]
- Saddle: SA-240, Type 304 [4b]
- Weld between Support Bracket and Saddle: 308SS [4b, 5 Attachment 3]
- Weld between Support Bracket and RPV: Alloy 182 [5, Attachment 3]

The vessel attachment information provided in Reference [5, Attachment 3] identifies that the bracket attachment weld may not have received a post weld heat treatment. Per General Electric specification 21A8702, the bracket and saddle may not be furnace sensitized [2].

The support bracket loads are taken from the vessel loading drawing, a NMP1 steam dryer repair design specification and the original stress analysis [8, 9, 7]. The original stress analysis contains a conservative assumption regarding eccentricity of the saddle on the support bracket such that a maximum moment arm is developed which would maximize stresses on the assembly. Further, the original stress analysis applies a conservative assumption of a friction coefficient of 1.0 and differential expansion of the vessel and dryer such that significant radial loads are created on the bracket by friction forces.

4.0 METHODOLOGY

The flaw evaluation documented in this report takes general guidance from BWRVIP-48-A [3] and the American Society of Mechanical Engineers (ASME) Boiler and Pressure Vessel Code (B&PV Code), Section XI, Appendix C [12]. The general flaw evaluation guidance given in BWRVIP-48-A [3] states simply that if a reportable indication cannot be accepted per the applicable acceptance criteria in ASME XI, IWB-3500 then a flaw evaluation must be performed using the methods of ASME XI, IWB-3600. ASME XI, IWB 3600 does not contain specific flaw evaluation procedures for vessel attachments. Consequently, the flaw evaluation methodology used for this evaluation, and documented below, follows the general format of the flaw evaluation procedures given in ASME XI, Appendix C. Since ASME XI, Appendix C does not contain specific formulae for solid components of rectangular cross-section, methods and solutions appropriate for the configuration are used, as described below.

The following items are described in this section:

- Loads
- Flaw Characterization
- NDE Uncertainty

- Crack Growth
- Failure Mechanisms
- Analysis Methods

4.1 Loads

Review of the original stress analysis and the steam dryer repair criteria given in BWRVIP-181 [13] suggest the following load combinations for the steam dryer support bracket:



Deadweight Load (DW)

The vessel loading drawing provides the DW [8]. The DW load considered in the original stress report [7] is used in the current evaluation. The DW loading does not consider buoyancy; this effect is considered to be negligible and it is conservative to ignore the effect since it acts to reduce the DW load. Further, the effect of buoyancy on the vertical load contributed on the support bracket following a MSL break event is considered to be negligible.

Seismic Load (OBE, SSE)

The vessel loading drawing provides the Seismic load [8]. No distinction is made between an Operating Basis Earthquake (OBE) load and a Safe Shutdown Earthquake (SSE) load. The seismic load considered in the original stress report [7] is considered in this evaluation.

Reactor Internal Pressure Differences (DP_N , DP_U , DP_F)

It is recognized that the Level A/B reactor internal pressure difference (RIPD) load will contribute a vertical load on the dryer which will act in the opposite direction to the DW load. The available steam dryer repair design specification does not specify separate Level A (Normal) and Level B (Upset) steam dryer RIPD loads; therefore, the value given in Section 4.2.3 of Reference [9] is used as both the Level A and Level B RIPD. Since the DP_N load given in Reference [9, Section 4.2.3], even when applied in a conservative manner, will create a force less than the DW load, the dryer will not lift. Consequently, the DP_N and DP_U loads are conservatively neglected for this evaluation. The conservative assessment of DP is shown below:

$$\text{Force}_{DP_N} = \pi(ID_{RPV})^2(DP_N) / 4 = \pi(209)^2(0.10)/4 = 3431 \text{ lbs}$$

$$\text{Force}_{DW} = 45,000 \text{ [4d]}$$

$\text{Force}_{DP_N} < \text{Force}_{DW}$ Therefore, dryer does not lift and Force_{DP_N} is conservatively neglected.

The RIPD created by the postulated Main Steam Line Break faulted event is discussed separately below.

Flow Induced Vibration Load (FIV)

FIV loads are fluctuating pressure loads which act upon the steam dryer surfaces and are caused by steam dome acoustics excited by various hydrodynamic mechanisms in the BWR steam system. No specific FIV load is currently defined for NMP1; therefore, no FIV load is considered in this analysis. Visual observation of the steam dryer support brackets does not show wear indicative of FIV. Validity of this assumption is discussed in more detail in Section 5.

Turbine Stop Valve Loads (TSV_A , TSV_F)

The loads caused by sudden closure of the turbine stop valves will be created in both main steam lines (MSL) since all TSV will close at the same time. These loads propagate back up the MSL then enter the steam dome through the main steam nozzles, where they act upon the steam dryer outer hoods. Both the acoustic and momentum loads will act essentially as symmetric loading on the dryer outer hoods which act to squeeze the dryer assembly but not to push the assembly down on the dryer support brackets with any significant loading. Consequently, these loads are not considered in the dryer support bracket flaw evaluation. This approach is consistent with the original stress analysis.

Main Steam Line Break Loads ($MSLB_A$, DP_F)

The MSLB event is a faulted event. The original NMP1 dryer analysis does not evaluate faulted events against specific allowable stress criteria; rather, adequacy of the dryer structure following a faulted event is assessed from a functionality perspective [21]. Essentially, if the dryer, which is not a safety related component, does not form loose parts following a faulted event, which would negatively impact the plant's ability to shut down safely, then the dryer is acceptable. The flaw evaluation documented in this analysis assesses functionality of the vessel bracket and considers an assumed MSLB pressure difference based upon available design information [2] which suggests the DP_F load would not exceed 2.0 psi.

Load Combinations for Flaw Evaluation

The following load combinations are considered in this flaw evaluation.

- Level A/B: DW + FIV + DP_U + OBE
- Level C/D: DW + DP_F + SSE

It should be noted that the structural factors required in Appendix C are lower for Level C/D events than for Level A/B events. Further, the DP_F will act in the opposite direction than DW; thus, the total vertical force resulting from the Level C/D load combination given above is:

$$V_{C/D} = DW - DP_F = 45000 - \frac{\pi(2)(209)^2}{4} = -23612 \text{ lbs}$$

The total dryer deadweight and diameter are given in Reference [4d]. Recognizing that the vertical force for the Level C/D load combination is less than that for the Level A/B load combination and that the required structural factor is less than for the Level A/B load combination, the Level A/B load combination will bound the Level C/D load combination. Only the Level A/B load combination will be considered in this evaluation.

Table 1 summarizes the loads identified for this evaluation. Figure 3 identifies the location of application for each load.

Table 1: Summary of Steam Dryer Support Bracket Loads.

Load	Value	Note
DW [7]	V = 15 kips F1 = 15 kips	F1 is the friction force assumed to be caused by differential thermal expansion
Seismic (OBE & SSE) [7]	H = 16.25 kips V = 3.75 kips F2 = 5 kips	F2 is the friction force assumed to be caused by differential thermal expansion
DP _N & DP _U [9]	0.04 psi minimum 0.10 psi maximum	
DP _F [2]	2.0 psi	Assumed sufficiently large to cause dryer to lift
FIV	-	Assumed negligible based upon IVVI results from bracket surfaces

4.2 Flaw Characterization

Since both UT and EVT-1 were used to perform the steam dryer support bracket inspections, the flaws are characterized using the reported lengths and depths from the UT report and separately characterized using the dimensions from the IVVI reports.

For the UT characterization, where the flaws are adjacent to un-inspected regions the flaw length was conservatively assumed to extend through the entire length of the uninspected region. The assumed flaws are given a depth equal to the adjacent crack depth. For the EVT-1 characterization no depth sizing information is available; therefore, all flaws are conservatively considered to be rectangular flaws where the legs of the rectangle are defined by the measured dimension of the flaw along the top/bottom surface of the bracket, and the left/right side of the bracket.

4.3 NDE Uncertainty

The length sizing uncertainty for EVT-1 is taken from BWRVIP-03[14] as reported for indications sized with a scale. Consequently, a sizing factor of { } inches is added to all dimensions reported in the IVVI inspection reports [1]. The U₁ sizing uncertainty is provided in the Design Input Request [2], as defined by the NDE vendor. A value of 0.050 inches is used for length sizing and 0.20 inches for depth sizing from the UT data.

4.4 Crack Growth

The flaws identified in the support brackets can grow from both fatigue crack growth (FCG) and stress corrosion crack (SCC) growth; therefore, both FCG and SCC growth are considered in this evaluation. The bounding SCC growth rate of 5E-5 in/hr for both stainless steel and Alloy 182 for normal water chemistry (NWC) conditions reported in BWRVIP-14-A [15] and BWRVIP-59-A [16], respectively, is used for this evaluation. Reduced SCC CGR cannot be applied because the steam dryer support bracket is not considered mitigated by Noble Metal Chemical Addition (NMCA) / Hydrogen Water Chemistry (HWC) [20].

The FCG rate correlations given in ASME XI, Appendix C [12c] for austenitic stainless steel in air and for Alloy 600 in a water environment are used for this evaluation. The FCG curves are taken from the 2010 Edition of the ASME Code since the 2004 Edition does not contain FCG

data for Alloy 600 materials. These data are well supported by the data presented in GEAP-24098 [19] which are for stainless steel and nickel alloys in simulated BWR coolant.

4.5 Failure Mechanisms

The indications reported in the steam dryer support bracket [1] all exist in the stainless steel base material in the Heat Affected Zone (HAZ) of the attachment weld. Both SA-240, Type 304 and Alloy 182 possess significant ductility in the unirradiated state. The failure modes typically considered for these materials are plastic collapse or ductile tearing. Since the dryer support bracket configuration is thick (2.5 inches in one direction and 8 inches in the other direction) this component may exhibit significant constraint. Materials that would otherwise fail in a ductile manner can fail in a more brittle manner when subjected to substantial constraint, because the constraint may prevent the material from displacing to develop the plasticity that it would otherwise be expected to exhibit. Consequently, brittle fracture is also considered as a possible failure mechanism for this component and is a conservative representation of the hypothetical failure of this component.

4.6 Analysis Methods

Since both plastic collapse and brittle fracture are considered as possible failure modes, analyses are specifically performed to address each of these failure mechanisms. The analytical methods used to perform the limit load and linear elastic fracture mechanics (LEFM) analysis for the Level A/B load case and the functional evaluation for the Level C/D load case are discussed separately below.

4.6.1 Limit Analysis

Review of the original stress report and the vessel loading drawing shows that the support bracket experiences loading which acts about multiple axes. Most lower bound collapse solutions available in the literature are applicable for configurations with uni-axial loading; therefore, no handbook collapse solution is considered applicable for this situation. Further, the steam dryer support bracket is a thick component in both axes; therefore, this component may experience significant constraint which would create a significant tri-axial stress state causing the possibility of a large hydrostatic stress which in turn would retard plastic flow. Components

which have significant constraint can fail in a more brittle manner even though they may be fabricated from normally ductile materials. Handbook collapse solutions derived assuming uni-axial loading do not inherently consider the possibility of developing hydrostatic stresses. Consequently, since both the multi-axial loading and the presence of constraint do not lend themselves to accurate analysis using handbook solutions a limit analysis is performed using the finite element method.

The ANSYS general purpose finite element analysis (FEA) software [17] is used for the limit analysis. The limit load is defined as that load which was applied to the structure at the last load step for which the ANSYS solution converged. Once the limit load is exceeded then the displacements in the finite element model increase without bound and the ANSYS solution cannot converge. An elastic-perfectly plastic material model is used for this analysis with the ANSYS bilinear isotropic hardening model. Implementation of this model requires a very small tangent modulus in order to enable convergence; therefore, the tangent modulus is defined as 100 psi. This value is sufficiently small that essentially no strain hardening is simulated. From the ANSYS manual [17], the following description of the bilinear isotropic material model is obtained:

This option (BISO) uses the von Mises yield criteria coupled with an isotropic work hardening assumption. The material behavior is described by a bilinear stress-strain curve starting at the origin with positive stress and strain values. The initial slope of the curve is taken as the elastic modulus of the material. At the specified yield stress (C1), the curve continues along the second slope defined by the tangent modulus C2 (having the same units as the elastic modulus). The tangent modulus cannot be less than zero nor greater than the elastic modulus.

The yield stress in the ANSYS BISO material model used for this analysis is defined as the flow stress of the material. The flow stress is defined consistent with ASME XI, Appendix C, paragraph C-8200 [12b]:

$$\sigma_f = \frac{\sigma_y + \sigma_u}{2} \quad (1)$$

Where: σ_f is the material flow stress, 40,850 psi
 σ_y is the material yield stress, 18,300 psi taken at 575 °F [7]

σ_u is the material ultimate stress, 63,400 psi taken at 550 °F [12a]

Material properties are taken from the original stress analysis [7] and ASME XI, Section II [12a] at 550 °F.

To demonstrate that this approach is accurate and acceptable for use in predicting the lower bound collapse load, a benchmark case is performed with a simple geometry for which a theoretical solution can be easily obtained. The benchmark case is performed for a thin rod subjected to an axial load.

The limit analysis of the steam dryer support bracket is performed with cracks present in the model. Cracks are simulated by defining two coplanar areas at the crack plane then merging all nodes not on the crack faces. In this manner the crack faces are free to separate in response to the applied loading. No crack tip elements are used along the crack front since the objective of the limit analysis is not to perform a finite element linear elastic fracture mechanics analysis.

Four elastic-plastic analyses are performed for this study as summarized in Table 2 below.

Table 2: Summary of Load Cases Evaluated for Level A/B Limit Analysis.

Load Case	Loads	Crack Case ¹	Mesh ²
1	Level A/B Multiplied by $SF_M=2.7$	UT-1	Baseline
2	Level A/B Multiplied by $SF_M=2.7$	Visual-1	Baseline (0.2 inch mesh)
3	Level A/B Multiplied by $SF_M=2.7$	Visual-1	Refined (0.1 inch mesh)
4	Level A/B Multiplied by $SF_M=2.7$	Visual-2	Baseline

Notes: 1. The crack cases are described in Figure 7.

2. The mesh utilized for the baseline case and the refined mesh are shown in Figures 12 and 13.

4.6.2 Linear Elastic Fracture Mechanics Analysis

Review of Figure 3 shows that a crack at the location identified in Figure 3 will experience membrane, bending, in-plane and out of plane shear, and torsional shear loading. Two fracture mechanics solutions are superposed in order to estimate the applied stress intensity factor for a conservatively assumed edge crack configuration in the support bracket. The solutions are shown in Figures 8 and 9. Review of the three crack configurations considered for this flaw evaluation, shown in Figure 7, shows that the single edge crack case, given as EVT-1 in Figure 7, defined using the visual data results in the most significant area reduction. This case is also considered to be the most conservative crack case for the LEFM analysis since it results in the largest crack. The other cases are essentially corner cracks which can be shown to produce substantially lower K_I results.

A fracture toughness of unirradiated stainless steel of $150 \text{ ksi-in}^{0.5}$ is taken from BWRVIP-14-A [15]. The bounding Level A structural factor for membrane loads, $SF_M=2.7$, is selected [12b]. Consequently, an allowable fracture toughness is obtained as:

$$K_{I_allowable} = \frac{K_{Ic}}{2.7} = \frac{150}{2.7} = 55.6 \text{ ksi-in}^{0.5} \quad (2)$$

Recognizing that Mode I, II, and III stress intensity factors are calculated and that the allowable fracture toughness is given for Mode I loading, an equivalent Mode I stress intensity factor is calculated using an equivalent energy release rate approach [18, pgs. 12-13]:

$$\wp = \frac{1-\nu}{2G} \cdot K_I^2 + \frac{1-\nu}{2G} \cdot K_{II}^2 + \frac{1}{2G} \cdot K_{III}^2 \quad (3)$$

Where: $E = 2 \cdot (1 + \nu) \cdot G$ (4)

\wp is the energy release rate,
 ν is the Poisson's ratio, dimensionless,
 E is the Elastic Modulus, psi,
 G is the Shear Modulus, psi.

Thus, an equivalent K_I may be approximated by calculating a total energy release rate then converting this back to an equivalent K_I which would give the same energy release rate. Combining Eqs. 3 and 4 gives:

$$K_{I_eq} = \sqrt{\frac{E}{1-\nu^2} \cdot \left(\frac{1-\nu^2}{E} \cdot K_I^2 + \frac{1-\nu^2}{E} \cdot K_{II}^2 + \frac{1+\nu}{E} \cdot K_{III}^2 \right)} \quad (5)$$

The effect of crack tip plasticity is included through the use of a plastic zone size correction factor as given in Reference [18, pg. 16]:

$$r_Y = \frac{1}{6\pi} \left(\frac{K}{\sigma_y} \right)^2, \text{ for plane strain} \quad (6)$$

$$a_{eff} = a + r_Y \quad (7)$$

Where:

- r_Y is the approximate radius of the plastic zone size, in
- K is the stress intensity factor (K_{I_eq} in this analysis), psi-in^{0.5}
- σ_y is the material yield strength, psi
- a is the flaw length, in
- a_{eff} is the effective flaw length, in

The cracked support bracket is considered acceptable for the evaluation interval if

$$K_{I_eq} < K_{I_allowable}$$

Consideration of the plastic zone size requires an iterative solution since the flaw length is a function of the applied K and the applied K is a function of the flaw length.

4.6.3 Functional Evaluation

The Level C/D load case is evaluated on a functional basis using criteria similar to those used in the original steam dryer evaluation. For the present evaluation, the RPV bracket is considered acceptable if its load carrying capacity is greater than the load carrying capacity of the steam dryer hold down assembly which is supported by the RPV bracket. Figure 22 illustrates the

configuration of the hold down assembly. Figure 23 is a photograph of the steam dryer hold-down assembly in the open position, without the vessel bracket inserted. Figure 23 is provided for informational purposes, in order to help communicate the configuration of this assembly. During a faulted event, the RIPD is assumed to be sufficiently large to cause the dryer to lift off the RPV bracket. In this case the bottom surface of the RPV bracket will experience an upward shear force and the swing arm assembly will experience a downward force which is reacted at one end by the lug shown in Figure 22 and at the other end by the circular rod about which the swing arm rotates.

4.6.4 *Qualitative Assessment of Radially Oriented Indication in 1-587A*

The radial indication in steam dryer support bracket 1-587A is evaluated in a qualitative manner since there are no loads on the bracket which would act to drive crack growth in this orientation.

4.6.5 *Method for Determining Allowable Flaw Size*

Since both LEFM and Limit Load evaluations are performed in this analysis, allowable flaw sizes considering both possible failure mechanisms are calculated. Two different crack configurations are considered. The methodology used for each is discussed separately below.

4.6.5.1 *Bounding Limit Load Method*

Two crack cases, given as UT Crack Case #1 and EVT-1 Crack Case #1 in Figure 7, are analyzed. Per Section 4.1, the Level A/B Load is the bounding load combination. The same FEM as described in Section 4.6.1 is used to evaluate the allowable flaw size for limit load. For this analysis the assumed crack size is incrementally increased until at least one of the three criteria below is violated. For the UT crack case #1, the crack size is incrementally increased using equal increments for all flaw dimensions, i.e., 1.477" vertical, 1.477" horizontal, 4.427" vertical, and 1.077" vertical in Figure 7. The largest flaw size at which all three criteria, listed below, are satisfied is defined as the allowable flaw size for limit load.

Three criteria are used to determine the allowable flaw size:

- The finite element analysis must converge. This criterion means the model with a given crack size can support the applied load.
- The Von Mises total strain (elastic + plastic) should be less than the elongation at rupture of 40% specified for SA-240, Tp. 304 [12a].
- The ASME Section III primary local membrane and local membrane plus bending stress intensity in the RPV shell should remain within the allowable value.

4.6.5.2 *LEFM Crack Case Evaluation*

Since the EVT-1 crack case, shown in Figure 7, is the most conservative configuration, it is considered for the LEFM allowable flaw size calculation. The LEFM allowable flaw size is determined using the same methodology as described in Section 4.6.2. For this calculation the crack size is incrementally increased until the calculated equivalent stress intensity factor equals the allowable fracture toughness. This is defined as the LEFM allowable flaw size.

5.0 ASSUMPTIONS

The following assumptions are used in this evaluation:

Geometry:

1. Distance between the toe of the Alloy 182 vessel attachment weld and the back side of the saddle is 0.25 inches.

Justification: CENG measured this distance from available inspection data for one bracket [11] as a distance between 0.09 and 0.12 inches. Recognizing that visual data was not obtained for the other two brackets with reportable indications a value of 0.25 inches is used in this evaluation and is considered representative of the nominal configuration.

2. Toe of the weld joining the saddle to the bracket is at the edge of the bracket.

Justification: The inspection photographs provided by CENG [1] confirm this orientation; thus, this assumption is supported by the as-built configuration.

3. Width of the steam dryer hold-down assembly swing arm is at least 2.0 inches.

Justification: The steam dryer drawings [4d] show the thickness of the swing arm as 2.375 inches. The drawings do not provide a dimension for the swing arm width. The available inspection photographs, see Figure 23, of the hold-down assembly suggest that the width of the swing arm is at least as large as the thickness. Based on the inspection data which shows the as-built configuration of one swing arm, it is considered acceptable to assume the width is at least 2.0 inches for the purposes of the Functional evaluation documented in this report.

4. Depth of the top surface of the saddle is not modeled with the two ¼ inch lips as shown in Figures 2 and 3; rather, the saddle is modeled as 2 inches wide at this surface.

Justification: This analysis applies the load in a manner consistent with the original stress analysis [7] in which the load is applied at the center of the saddle surface. Consequently, presence of the two lips have no effect on the transfer of the load from the saddle to the bracket. The evaluation is concerned with stability of the bracket rather than the saddle; therefore, this simplifying assumption is considered to be acceptable.

5. Width of the saddle is increased by 0.25 inches on one side of the bracket in order to incorporate an eccentricity similar to that considered in the original stress analysis [7].

Justification: This modeling assumption is applied in a manner similar to the original support bracket stress analysis [7]. Implementing the eccentricity in the applied loading by increasing the width of one leg of the saddle does not affect the load carrying capacity of the bracket; rather, it simply causes the location of the equivalent load to be shifted by 0.125 inches to one side. Consequently, this modeling assumption is considered to be acceptable.

Loads:

1. There are no significant flow induced vibration (FIV) loads acting on the support brackets.

Justification: The available inspection data show two wear spots on the top surface of the saddle. These wear spots are not indicative of sustained vibration caused by a high cycle fluctuating load caused by FIV. Loads of this nature have been observed to cause wear in steam dryer support brackets in other BWRs. In these cases the

brackets have exhibited substantial wear (on the order of 0.125 to 0.25 inches) into the depth of the bracket. At NMP1 the surface oxide layer is removed; however, the overall level of the saddle has not changed; thus, the assumption of no significant FIV loads is justified.

2. The magnitude of the MSLB RIPD will not exceed 2.0 psi.

Justification: Design data provided by CENG in the Design Input Request [2] shows that a maximum MSLB DP of 2.0 psi is expected.

3. Installation of the steam dryer assembly does not contribute a significant fatigue loading or cycles to the steam dryer support bracket.

Justification: Based upon input provided by CENG the dryer is installed with substantial caution to avoid impact loading on the steam dryer support bracket.

Material:

1. The hold-down assembly in the NMP1 steam dryer is Stainless Steel type 304.

Justification: BWR steam dryers are fabricated from stainless steel. Typical material types for steam dryer components are Type 304; therefore, this is assumed for this analysis.

6.0 CONSERVATISMS

Although the methodology utilized for this flaw evaluation is considered to be consistent with the guidance of ASME XI, IWB-3600, it is acknowledge that the component evaluated in this analysis does not clearly fall under the existing flaw evaluation rules given in ASME XI, Appendix C. Consequently, this section is included to clearly identify some of the conservatism inherent in the methodology used.

1. The Level A/B RIPD is neglected which is conservative since this load acts opposite to DW. This increases the load considered in the evaluation.

2. A friction coefficient of 1.0 is assumed such that substantial axial loading is introduced into the bracket, consistent with the original stress analysis.
3. The bounding, K-independent, NWC, IGSCC crack growth rate is applied for crack growth.
4. A linear elastic fracture mechanics analysis is performed to assess the likelihood of unstable crack propagation in the bracket as opposed to a more complex but more appropriate and less conservative elastic-plastic fracture mechanics analysis.
5. A bounding Level A structural factor for membrane loads is considered for all loading (membrane, bending, shear) and for the limiting load combination which considers Level B loads.
6. A conservative end-of-evaluation interval crack distribution was selected based upon conservative treatment of visual data despite the fact that the available UT data supports consideration of a less conservative crack distribution.
7. Fatigue crack growth is assessed by treating all load cycles to consist of both a full DW and Seismic contribution despite the fact that for a seismic event the deadweight would act as a mean load rather than a direct contributor to the ΔK .
8. An R-ratio of 0.9 is used for the FCG assessment despite the fact that the R ratio is shown to be closer to 0.5.
9. An edge cracked LEFM model is selected based on the visual data despite the fact that the UT data support characterization of the flaws as corner cracks.

7.0 ANALYSIS

The following steps of the analysis are described in this section:

- Flaw Characterization and Summary
- Flaw Growth (NDE Uncertainty and Crack Growth)
- LEFM Analysis
- Limit Analysis
- Functional Analysis
- Qualitative Assessment of Radial Indication in 1-587A
- Allowable Flaw Sizes

7.1 Flaw Characterization and Summary

The flaw sizing information contained in the visual and UT inspection reports for the 1-587A, B, and C support brackets are presented in Figure 4. This figure identifies the uninspected regions for the UT examination. Figure 5 shows the initial flaw sizes for the EVT-1 and UT data, separately, without considering the appropriate non-destructive examination uncertainty. The initial flaw sizes are determined as described in Section 4.2 above. NDE sizing uncertainty is included with the flaw growth and is discussed in Section 7.2 below.

7.2 Flaw Growth

The initial flaw sizes shown in Figure 5 are increased to account for NDE uncertainty as well as crack growth from fatigue and stress corrosion cracking. The evaluation interval selected for this flaw evaluation is one fuel cycle (2 years).

From BWRVIP-03 [14], the appropriate evaluation factor for EVT-1 for measurement by ruler is { } inches. Each dimension of every flaw is increased by { } inches prior to calculation of crack growth. As obtained from the UT vendor, a UT depth sizing factor of 0.2 inches is used and a UT length sizing factor of 0.05 inches is used [2].

Intergranular stress corrosion crack (IGSCC) growth is considered using the bounding, K-independent, Normal Water Chemistry (NWC), crack growth for both the stainless steel base material and the Alloy 182 weld material reported in BWRVIP-14-A [15] and BWRVIP-59-A [16]. This value is $5E-5$ in/hr. The total IGSCC growth added to each flaw tip for the evaluation interval is:

$$\Delta a_{SCC} = 365.5 \cdot 2 \cdot 24 \cdot 5 \times 10^{-5} = 0.877 \text{ in / tip}$$

Fatigue crack growth (FCG) is calculated assuming:

- 6 Startup/shutdown cycles (3 cycle per year)
- 5 Seismic cycles (1 event with 5 cycles assumed for the event)

The entire load (both DW and Seismic) considered in the original stress report is conservatively assumed to act for both the startup/shutdown and seismic events; thus, 11 cycles are considered. The K_{IEQ} calculated in the LEFM section below is treated as the range of stress intensity factor

(ΔK_I) used for the FCG calculation. This assumption considers that the loads cycle from a no load condition (i.e. dryer removed) to the full load (dryer installed and seismic event) which is a reasonable assumption for the startup/shutdown load and conservative for the seismic load since for the seismic event the DW loads would act as mean loads. For this calculation, the effect of residual stresses is to increase the R-ratio but has no effect on the ΔK ; therefore, an R-ratio near 1.0 will be conservatively assumed in order to maximize the effect of mean stresses. Further, the LEFM evaluation described in Section 7.1.3 assumes an edge crack rather than a part through-wall crack; therefore, the K_I results used for this evaluation are very conservative.

Considering a $\Delta K_I = 27.1 \text{ ksi-in}^{0.5}$ the FCG rate for Alloy 600 at 600 °F, with a R-ratio of 0.9 from Figure C-8410-2 of ASME XI, Appendix C, 2010 Edition [12c] is $da/dn = \sim 1.5E-4$ in/cycle. No FCG curves for austenitic stainless steel in water are currently available in the ASME Code; however, noting the similarity between the air FCG curves for Austenitic stainless steel and Alloy 600, and that the air and water curves for the Alloy 600 converge for $\Delta K > 20 \text{ ksi-in}^{0.5}$, the air FCG rate from Figure C-8410-1 of ASME XI, Appendix C, 2010 Ed. [12c] for 550 °F and a R-ratio of 0.9 is used. Consequently, the FCG rate for the austenitic stainless steel base material, $da/dn = \sim 1.5E-4$ in/cycle. An R-ratio of 0.9 is considered acceptable and conservative since the applied stresses, given in the original stress report [7], are on the order of 16 ksi and the yield stress of the material at operating temperature is on the order of 18 ksi (the weld residual stress is conservatively assumed to be at yield); thus, since the applied stress intensity factor is proportional to stress, the R-ratio can be estimated as $16/(18+16)=0.47$. The crack growth rates described above are well supported by the data published in GEAP-24098 [19] prepared by General Electric under contract to the Nuclear Regulatory Commission (NRC). Finally, the calculated FCG for the evaluation interval, conservatively calculated assuming the edge cracked LEFM solution described above and that all SCC crack growth has occurred first (i.e. results in a larger ΔK_I) is given as:

$$\Delta a = 11 \cdot 1.5 \times 10^{-4} = 0.0017 \text{ inches}$$

This value would be added to each dimension of each flaw. Considering that this value is almost negligible and that the assumptions for crack size, LEFM solution, and loading are extremely

conservative, this value is considered to be an upper bound. Consequently, FCG is considered to be insignificant for the evaluation interval.

Considering the flaws defined in Section 7.1, the NDE sizing factors, and the IGSCC growth calculated in this section, the end of evaluation interval flaw sizes considered for this flaw evaluation are shown in Figure 6.

Figure 7 shows the three crack cases evaluated in this analysis for the limit analysis. Even though volumetric data is available two additional crack cases based only on the conservative treatment of the visual data are defined and evaluated.

7.3 Linear Elastic Fracture Mechanics Analysis

Appendix A contains the LEFM calculations performed in MathCAD. Table 3 presents the results of the LEFM evaluation. Per Section 4.6.2, an iterative solution is applied to calculate the plastic zone correction size with the end of evaluation interval flaw size of 4.327 inches, shown in Figure 7. The plastic zone size correction is 0.123 inches. Section 7.7.2 contains the results of the allowable flaw size analysis.

Table 3: Summary of LEFM Evaluation.

Case	See Figure 9		See Figure 8		K _{IEQ} , ksi-in ^{0.5}	K _{I Allow} , ksi-in ^{0.5}	Acceptable
	K _I , ksi-in ^{0.5}	K _{II,1} , ksi-in ^{0.5}	K _{II,2} , ksi-in ^{0.5}	K _{III} , ksi-in ^{0.5}			
EVT-1 Crack Case #1	11.17	3.17	4.56	20.34	27.85	55.6	Yes

7.4 Limit Analysis

Validity of the method used to simulate collapse in a structure using ANSYS was confirmed by performing a benchmark analysis. The benchmark was performed for a 1 inch diameter slender rod loaded in axial tension. The ANSYS SOLID95 element type is used for this simulation. A mesh size of 0.1" is defined and a flow stress of 47.5 ksi and Young's Modulus of 30E6 psi are arbitrarily selected. The theoretical lower bound limit load for this geometry is given as:

$$P_c = \frac{\pi \cdot OD^2}{4} \cdot \sigma_f = \frac{\pi \cdot 1^2}{4} \cdot 47500 = 37305 \text{ lbs.}$$

Figure 10 illustrates the FEM with the applied loads and boundary conditions. One end of the rod was fixed in all degrees of freedom (DOF) and the other end was loaded in tension with the theoretical collapse load, 37,305 lbs. The last converged solution time step was $t=0.99812$ which corresponds to a load of $0.99812 (37,305 \text{ lbs}) = 37,235 \text{ lbs}$. Review of the ANSYS reaction solution shows that the reaction loads are 37,236 pounds at the last converged time step. Figure 10 also shows the maximum elastic principal strain and the principal stress at $t=0.99812$. Both of these plots show that the rod is just reaching collapse. These results show that the ANSYS numerical prediction for the collapse load of the rod is within 0.2%, as shown below:

$$\%Error = \frac{(37236 - 37305)}{37305} \cdot 100 = -0.18\%$$

Had a smaller minimum time step been defined, the accuracy of the numerical solution could have been shown to be greater; however, for the purposes of this benchmark, an error of less than 0.2% is considered to be acceptable. Consequently, the element type, mesh size, and methodology of predicting collapse loads using ANSYS is considered benchmarked and acceptable for use for this flaw evaluation.

Figure 11 shows the FEM built to perform the limit analysis of the steam dryer support bracket. Dimensions for the support bracket and RPV were taken from the RPV drawings [4]. The width of the saddle was increased by 0.25 inches on the right side in order to introduce an eccentricity to the loading similar to that considered in the original stress report [7]. The material yield strength used in the original stress report [7] was used for this analysis. The ultimate strength and Elastic Modulus at 550 °F were taken from Reference [12a]; thus, the flow stress used as the “yield” point in the ANSYS FEM is $(18.3+63.4)/2=40.85 \text{ ksi}$. Loads were applied uniformly over the top and right sides of the saddle as summarized in Table 1 and Figure 3. The loads in Table 1 were increased by the maximum Level A/B structural factor, 2.7, given in ASME XI, Appendix C [12b] in order to evaluate if the cracked configuration of the bracket, at the end of the evaluation interval, retained the required minimum structural margin against collapse. The SOLID95 element type was used for this analysis. Both a 0.1 and a 0.2 inch mesh size were separately used in order to assess adequacy of the mesh density used in the analysis. To model the membrane stresses in the RPV contributed by the vessel internal pressure, a pressure load is applied to the top and left surfaces of the simulated RPV wall. The pressure loads are defined

equal to the axial (7500 psi) and hoop (15000 psi) stresses in the RPV as calculated using thin shell equations. The bottom surface of the simulated RPV wall was fixed in the Y direction, the right side was fixed in the X direction, and the outside surface of the RPV was fixed in the Z direction. The global coordinate system is shown in all figures showing the FEM and results. Figures 11, 12, and 13 show the finite element mesh for both mesh cases as well as the boundary conditions applied for the analyses. Figure 15 shows the Von Mises stress for the crack case EVT-1, Mesh Size 0.1 inches. The EVT-1 crack case is seen to be the limiting case of the three cases considered. Figures 16 through 19 show the Von Mises stress, Hydrostatic Stress, Maximum Principal Stress, and Von Mises Total Strain, respectively on the crack plane for both the 0.2 and 0.1 inch mesh sizes for the EVT-1 crack case. Figures 20 and 21 show the Von Mises stress, Von Mises strain, maximum principal stress, and hydrostatic stress for the UT-1 and EVT-2 Crack Cases, respectively, for a Mesh Size of 0.2 inches. These results show the following items:

1. The mesh density of 0.1 inches is acceptable for this evaluation based on the benchmark study and the good agreement between the results for the 0.2 and 0.1 inch mesh cases for the EVT-1 crack case (Figures 16-19).
2. The EVT-1 crack case is the limiting crack case of the three defined in Figure 7 (Compare Figures 16, 20, and 21). Although regions of the crack plane have reached the flow stress, there remains an elastic core in the uncracked material (Figure 16) which shows there remains additional margin before collapse.
3. There are significant Hydrostatic stresses on the crack plane (Figure 17) which result in principal stresses which are far greater than the uni-axial flow stress (Figure 18). This suggests substantial constraint which would inhibit plastic flow and supports the consideration of brittle fracture as an additional failure mechanism for this component.
4. The Von Mises total strain (Figure 19) of approximately 6% is significantly less than the elongation at rupture of 40% specified for SA-240, Tp. 304 [12a].
5. The steam dryer support brackets retain the required structural margin against collapse at the end of the evaluation interval.

7.5 Functional Analysis

Figure 22 illustrates the load path for the Faulted load case in which the steam dryer lifts off the vessel bracket and is retained by the swing arm of the hold-down assembly. For this load case an upward vertical load is applied to the vessel bracket which is reacted by a downward vertical load on the swing arm of the hold-down assembly. As shown in Figure 22, the load imparted to the swing arm from the vessel bracket is reacted by the lug on the right side and the vertical rod on the left side. Since data regarding the actual position of the vessel bracket on the swing arm, between the two reaction points is not known, it is assumed for this analysis that the bracket is located at the midpoint of the swing arm. Considering this, the vertical rod and the lug will each react $\frac{1}{2}$ of the vertical load imparted by the vessel bracket.

Since the swing arm is loaded in shear it will be considered to fail in shear. Since the rod takes the load in tension it will be considered to fail in tension. The vessel bracket is loaded in shear for this load case; therefore, the vessel bracket will fail in shear. Both the steam dryer assembly and the vessel bracket are stainless steel; therefore, they will be treated as having the same flow stress for this evaluation.

Review of Reference [4d] gives the thickness of the swing arm shown in Figure 22 as 2 -3/8 inches. Although the width of the swing arm is not given in any of the available references, based on the available inspection photographs, it is assumed that the width of the swing arm is at least 2.0 inches. This gives a cross-sectional area of the swing arm of $2.375(2) = 4.75 \text{ in}^2$.

Review of Reference [4d] gives the diameter of the vertical rod in the hold-down assembly as 1.5 inches. This gives a tensile area of $\pi(1.5^2)/4 = 1.77 \text{ in}^2$.

Review of Reference [4b] gives the dimensions of the steam dryer support bracket as 2.5 in. x 8 in. Considering the end of evaluation interval crack profile given in the EVT-1 crack case identified on Figure 7, the available end of interval shear area is $2.5(8-4.327) = 9.18 \text{ in}^2$.

Considering that the collapse load of a section loaded in tension or shear is given by $P_c = \sigma_f A$, where σ_f is the tensile or shear flow stress and A is the tensile or shear area, and that the shear flow stress is taken as $\frac{1}{2}$ of the tensile flow stress, the collapse loads for each component are:

Vessel Bracket	$P_c=9.18\sigma_f/2 = 4.59\sigma_f$
Hold-down Rod	$P_c=1.77\sigma_f$
Swing Arm	$P_c=4.75\sigma_f/2 = 2.38\sigma_f$

Finally, recognizing that the load carrying capacity of the vessel bracket must be at least twice as large as that of the hold-down rod since the rod will only react ½ of the load imparted by the bracket, it is seen above that the collapse load of the vessel bracket, considering the end of evaluation interval flaw distribution is greater than that of the swing arm and is greater than twice that of the hold-down rod; therefore, the bracket is considered acceptable for Level C/D loading since the strength of the bracket is greater than that of the dryer hold down assembly.

7.6 Qualitative Assessment of Radial Indication in 1-587A

Based upon the location (in vessel, and on bracket), local environment, materials, and available IVVI data it is expected that the indication is likely the result of IGSCC (or TGSCC) initiating and subsequently propagating intergranularly from a cold work induced surface layer on the bracket that was produced during the initial fabrication process. Operating experience has demonstrated that the cold worked layer is typically shallow. Further, there are no significant mechanical or thermal loadings acting on the bracket which would contribute a significant load normal to the crack face. Closer to the vessel attachment weld there are expected to be weld residual stresses which may contribute to crack growth.

Taking the initial flaw size as 0.875 inches [1] and adding the appropriate NDE uncertainty of { } inches [14] then adding one cycle of IGSCC growth, using the bounding SCC crack growth rate discussed in Section 7.2 above, yields an end-of-interval flaw size of 1.952 inches. The available design drawings for the bracket do not provide a dimension between the free surface of the bracket and the RPV; however, the inspection data contained in the design input request [2] shows that the as-built dimensions of the brackets are on the order of 3.3 inches to the toe of the weld and 4.0 inches to the inside surface of the RPV clad. Thus, the end-of-interval flaw size of the radially oriented indication will remain approximately 2 inches from the ferritic material of the RPV. Recognizing that this indication will remain approximately 1 inch from the toe of the Alloy 182 attachment weld, even considering the bounding SCC crack growth rate, there are not

expected to be significant residual stresses acting on this flaw. Recognizing that there are no credible operating load which would contribute FCG or which would contribute to fracture or collapse of the bracket in a direction normal to this crack orientation, this flaw is considered to be acceptable without detailed evaluation.

7.7 Allowable Flaw Sizes

7.7.1 Limit Load Allowable Flaw Sizes

Based on the methodology in Section 4.6.5.1, the FEM built in Section 4.6.1 is used to evaluate both the UT #1 and EVT-1 #1 crack cases considering several crack lengths and mesh densities. Table 4 summarizes the converged flaw size results.

Considering the acceptance criteria, the allowable flaw size for the EVT-1 #1 crack configuration is shown to be 4.6 inches. From Section 7.2, the IGSCC growth considering one operating cycle (two years) is 0.877 inches. Therefore, considering an allowable flaw size for the EVT-1 #1 crack case of 4.6 inches, the acceptable flaw size, considering a one cycle evaluation interval, is $4.6 \text{ in.} - 0.877 \text{ in.} = 3.72 \text{ inches}$. Figure 24 shows the allowable flaw size for the EVT-1 #1 crack case.

Considering that the UT #1 crack case is complex and requires four dimensions to describe the crack configuration, the allowable flaw size results reported in Table 4 and discussed here are presented in the context of an additional increment in flaw size from the dimensions given in Figure 7. The allowable incremental increase in flaw size, in each direction, for the UT #1 crack case is 0.3 inches; therefore, the acceptable flaw size, considering a one cycle evaluation interval, is 0.877 inches less than the dimensions shown in Figure 24

Table 4: Summary of Allowable Flaw Size under Bounding Limit Load.

Crack Case	Flaw Size (in.)	Mesh Density	Total Mechanical von Mises Strain (%)	Maximum Linearized Stress at Vessel (ksi)		Allowable Stress (ksi)	
				Local Membrane	Local Membrane Plus Bending		
EVT-1 #1	4.9	0.2	15513	Local Membrane	17.73	26.7 * 1.5 = 40.05	
				Local Membrane Plus Bending	21.94		
	4.65	0.1	66.23	Local Membrane	17.64		
				Local Membrane Plus Bending	20.63		
	4.60	0.1	21.90	Local Membrane	17.68		
				Local Membrane Plus Bending	20.73		
	4.55	0.1	9.51	Local Membrane	17.69		
				Local Membrane Plus Bending	20.79		
	4.35	0.1	5.94	Local Membrane	17.63		
				Local Membrane Plus Bending	20.59		
	UT #1	0.35 ¹	0.1	131.40	Local Membrane		16.21
					Local Membrane Plus Bending		16.71
0.3 ¹		0.1	14.32	Local Membrane	16.14		
				Local Membrane Plus Bending	16.76		
0.2 ¹		0.1	6.16	Local Membrane	16.12		
				Local Membrane Plus Bending	16.75		

Note: 1. These values are equal increments, added to the flaw dimensions given in Figure7. A single dimension is not reported here since this crack configuration is described by four dimensions.

7.7.2 LEFM Allowable Flaw Size

Based on the method in Section 4.6.5.2, the LEFM allowable flaw size evaluation is performed using MathCAD, as described in Section 7.3. The allowable flaw size, for the EVT-1 #1 crack case is calculated to be 5.92 inches with a plastic zone size correction of approximately 0.484 inches. Since the support bracket height is 8 in., the remaining ligament is 8 in. – 5.92 in = 2.08

in. Comparing the remaining ligament, 2.08 in., with the radius of the plastic zone, 0.484 in. (plastic zone is approximately 0.968 in.) shows that the region of plasticity is a significant portion of the remaining ligament. The large plastic zone size suggests that the inherent assumptions in linear elastic fracture mechanics (small region of crack tip plasticity) are violated and that LEFM is likely not the anticipated failure mechanism for this material and configuration. Consequently, a similar LEFM evaluation is not performed for the UT #1 crack case to determine a LEFM based allowable flaw size.

7.7.3 Summary of the Allowable Flaw Sizes

Since the results from LEFM analysis are shown to be not applicable because of the large region of crack tip plasticity, the FEM limit load allowable flaw sizes are considered to be the appropriate values to use. Figure 24 shows the end of interval allowable flaw size. Flaw sizing data acquired during a future inspection must have inspection uncertainty and crack growth added to it before comparison to the allowable flaw sizes shown in Figure 24. It should also be noted that this evaluation conservatively used a IGSCC growth rate of $5E-5$ inches/hour; however, per BWRVIP-14-A [15] a depth crack growth rate of $2.2E-5$ inches/hour may be applied for growth in the depth direction if the conductivity requirements given in BWRVIP-14-A [15] are satisfied. The length crack growth rate of $5E-5$ inches/hour cannot be reduced.

8.0 CONCLUSIONS

The results of the flaw evaluation documented in this report support the following conclusions and recommendations:

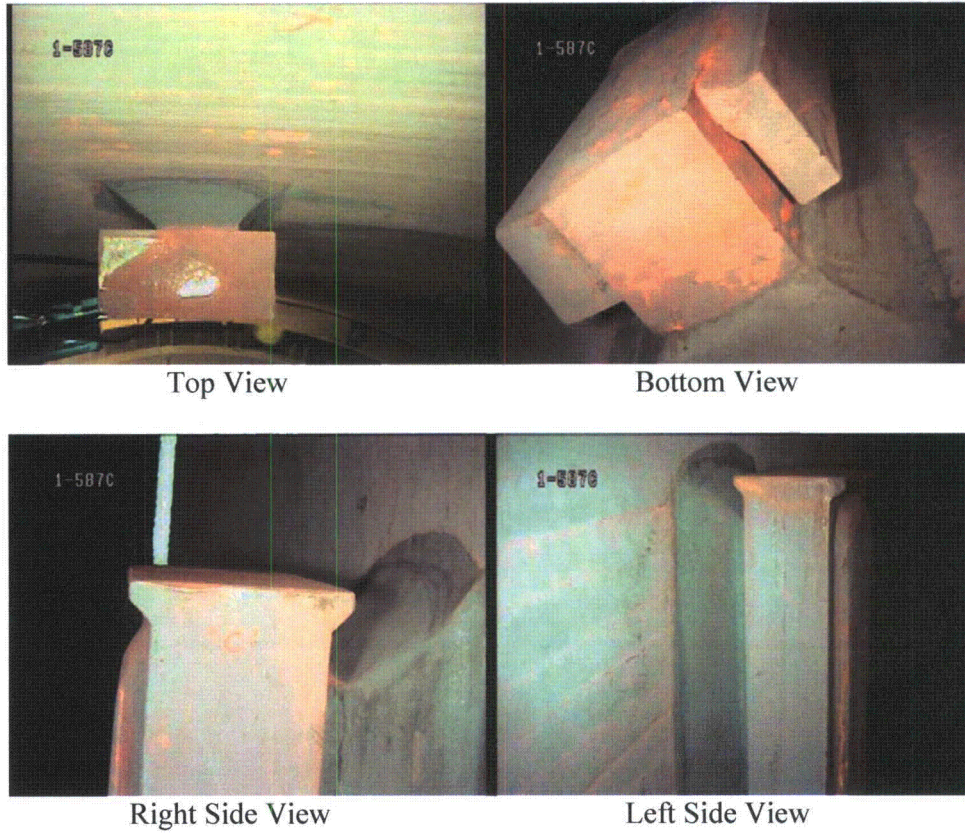
1. The indications reported in the NMP1 steam dryer support brackets 1-587A, 1-587B, and 1-587C are acceptable, as-is, for at least one additional cycle of operation.
2. SI recommends that CENG re-examine all four steam dryer support brackets using a qualified volumetric inspection technique during the next refueling outage to confirm behavior of the flaws remains bounded by the flaw growth evaluation documented in this report.

3. SI recommends that CENG consider a contingency repair option during the next refueling outage.
4. The NMP1 steam dryer support bracket allowable flaw sizes for crack configurations given by EVT-1 crack case #1 and UT crack case #1 (See Figure 7), considering both limit load and LEFM, are shown in Figure 24. In both cases the allowable flaw size is greater than the predicted end of evaluation interval flaw size.

9.0 REFERENCES

1. Westinghouse Indication Notification Forms, SI File No. 1100539.204:
 - a. NMP1-RFO-21-INF-11-15R2, April 2, 2011
 - b. NMP1-RFO-21-INF-11-16, March 30, 2011
 - c. NMP1-RFO-21-INF-11-19R3, April 4, 2011
2. Design Input Request, Rev. 3, SI File No. 1100539.201.
3. BWRVIP-48-A: BWR Vessel and Internals Project, Vessel ID Attachment Weld Inspection and Flaw Evaluation Guidelines, EPRI, Palo Alto, CA: 2004. 1009948.
4. Steam Dryer Drawings, SI File No. 1100539.202:
 - a. Niagara Mohawk Drawing 104R859, Arrangement and Assembly Reactor.
 - b. Combustion Engineering, Inc. Drawing 231-587, Rev. 3, Internal Attachments.
 - c. General Electric Drawing, 237E433, Sht. 4, Reactor Vessel.
 - d. Niagara Mohawk Drawing 706E293, Sht. 1, Rev. 5, Reactor Steam Dryer.
5. Vessel ID Attachment Weld Inspection and Evaluation, NER-1M-078, Rev. 2, SI File No. 1100539.207
6. Combustion Engineering Drawing, 231-563, Rev. 8, Vessel Forming and Welding Upper, SI File No. 1100539.202.
7. Combustion Engineering Report No. CENC-1142, NMP Calc. No. S0VESSELM026, SI File No. 1100539.206.
8. General Electric Drawing, 237E434, Sht. 1, Rev. 5, Reactor Vessel, SI File No. 1100539.209.
9. General Electric Design Specification, Steam Dryer, 23A1624, Rev. 1, SI File No. 1100539.209.
10. Inspection Photographs of NMP1 Steam Dryer Support Bracket, SI File No. 1100539.204.
11. Dimensions Estimated from Inspection Photographs of NMP1 Steam Dryer Support Bracket, SI File No. 1100539.210.
12. American Society of Mechanical Engineers Boiler and Pressure Vessel Code:
 - a. Section II, 2004 Ed., No Addenda.
 - b. Section XI, 2004 Ed., No Addenda.
 - c. Section XI, 2010 Ed., No Addenda.
 - d. Section III, 2004 Ed., No Addenda.
13. BWRVIP-181: BWR Vessel and Internals Project, Steam Dryer Repair Design Criteria. EPRI, Palo Alto, CA: 2007. 1013403.

14. TR-105696-R11 (BWRVIP-03) Revision 11: BWR Vessel and Internals Project, Reactor Pressure Vessel and Internals Examination Guidelines. EPRI, Palo Alto , CA: 2008. 1016584.
15. BWRVIP-14-A: BWR Vessel and Internals Project, Evaluation of Crack Growth in BWR Stainless Steel RPV Internals, EPRI Report 1016569, September 2008.
16. BWRVIP-59-A: BWR Vessel and Internals Project, Evaluation of Crack Growth in BWR Nickel Base Austenitic Alloys in RPV Internals. EPRI, Palo Alto, CA: 2007. 1014874.
17. ANSYS Mechanical and PrepPost, Release 11.0 (w/Service Pack 1), ANSYS, Inc., August 2007.
18. Tada, Hiroshi, Paris, Paul C., Irwin, George, R., The Stress Analysis of Cracks Handbook, 3rd Ed., ASME Press, 2000.
19. Hale, D.A., Yuen, J., Gerber, T., "Fatigue Crack Growth in Piping and RPV Steels in Simulated BWR Water Environment," GEAP-24098, January 1978, General Electric.
20. "BWRVIP-219: Technical Basis for On-Line NobleChem™ Mitigation and Effectiveness Criteria for Inspection Relief, EPRI Technical Report 1019071, July 2009.
21. NMP1 Final Safety Analysis Report (Updated), Revision 21, Chapter IV, Section 7.2. SI File 1100539.211.



Note: The photographs used here are from 1-587C.

Figure 1. Photographs of NMP1 Steam Dryer Support Bracket Configuration [1].

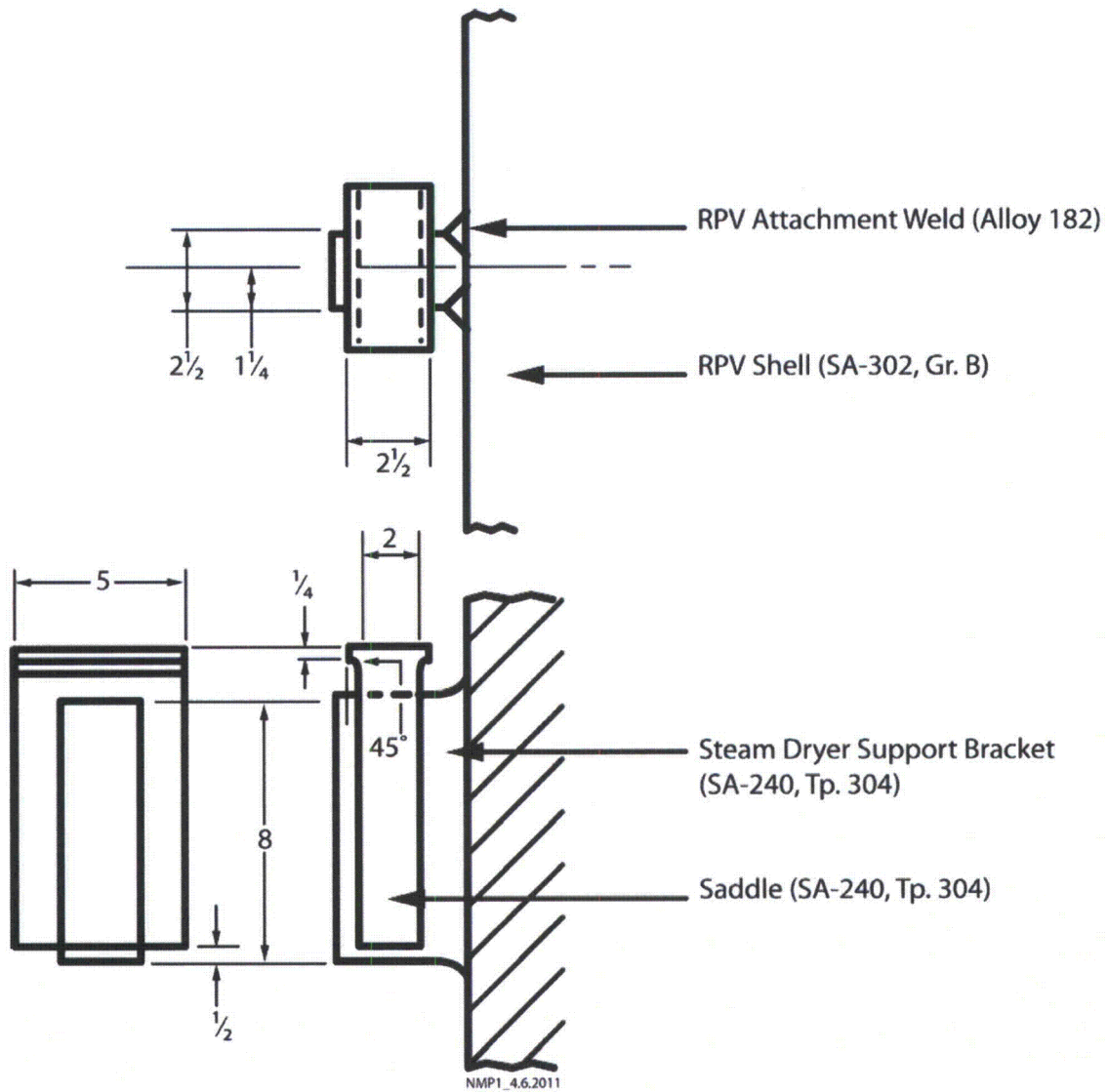
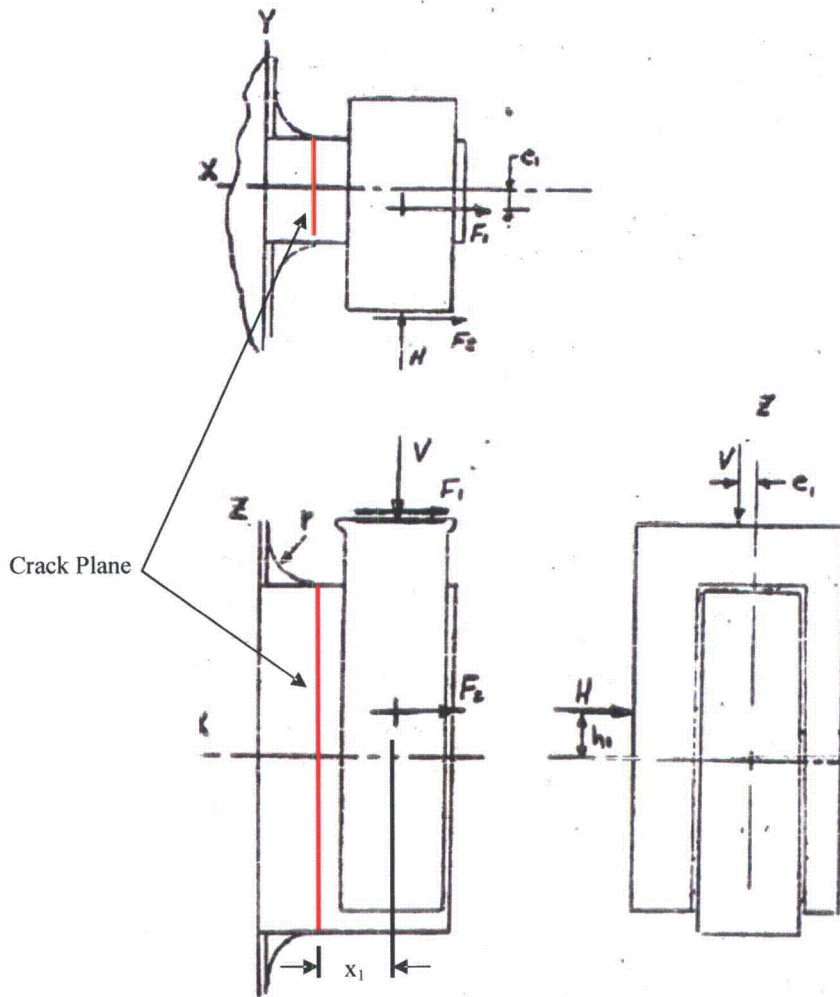
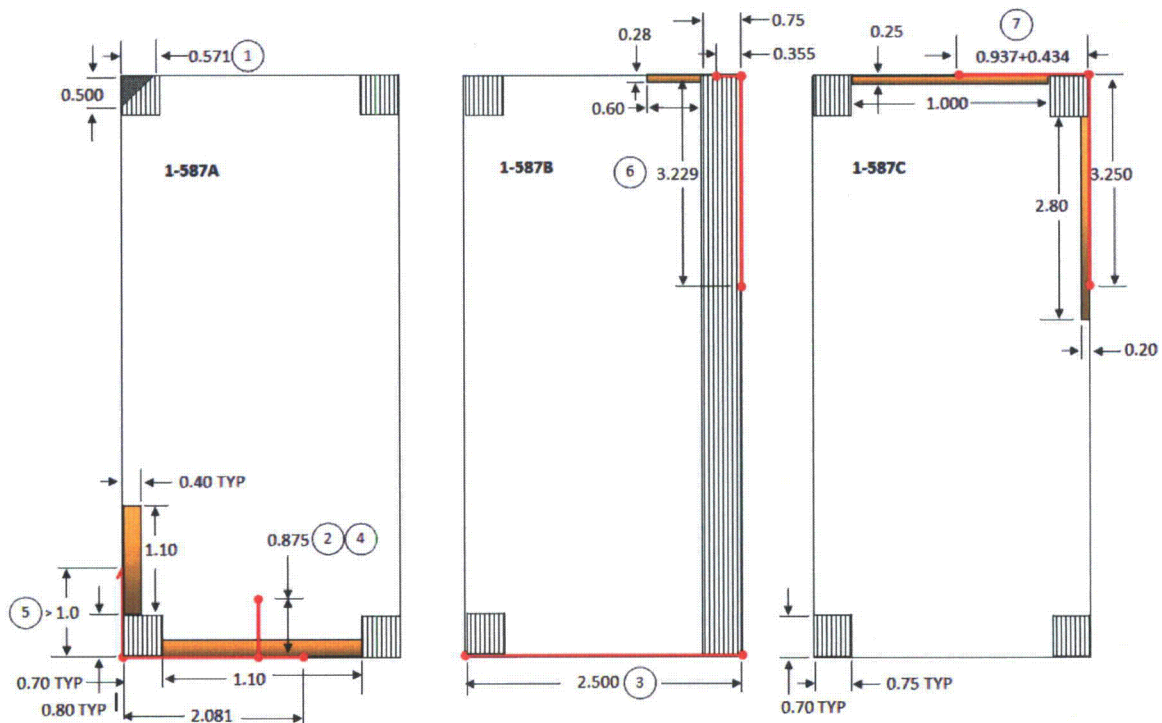


Figure 2. Schematic of Steam Dryer Support Bracket Configuration.



Note: $e_1 = 0.125$ inches
 $h_1 = 1.0$ inches
 $x_1 = 1.25$ inches

Figure 3. Schematic Illustrating Location of Applied Loads on Steam Dryer Support Bracket.



-  UT Uninspectable regions
-  UT Indication
-  EVT-1 Indication

- Notes:
- (1) Damage to front corner of support bracket shown in INF-11-19R3 [1c]. This is not on the same plane as the indications near the attachment weld.
 - (2) Flaw detected by EVT-1 on bottom front surface of bracket. This is not on the same plane as the indications near the attachment weld.
 - (3) This indication was not detected by UT.
 - (4) This indication was not detected by UT.
 - (5) The end of this indication was not discernable by EVT-1. The indication appeared to run underneath the saddle.
 - (6) This indication was not detected by UT because no UT scans were performed which could interrogate this region.
 - (7) The length of this indication is defined by summing the length of the both branches reported in INF-11-15R2 [1a].

Figure 4. Overlay of Inspection Data.

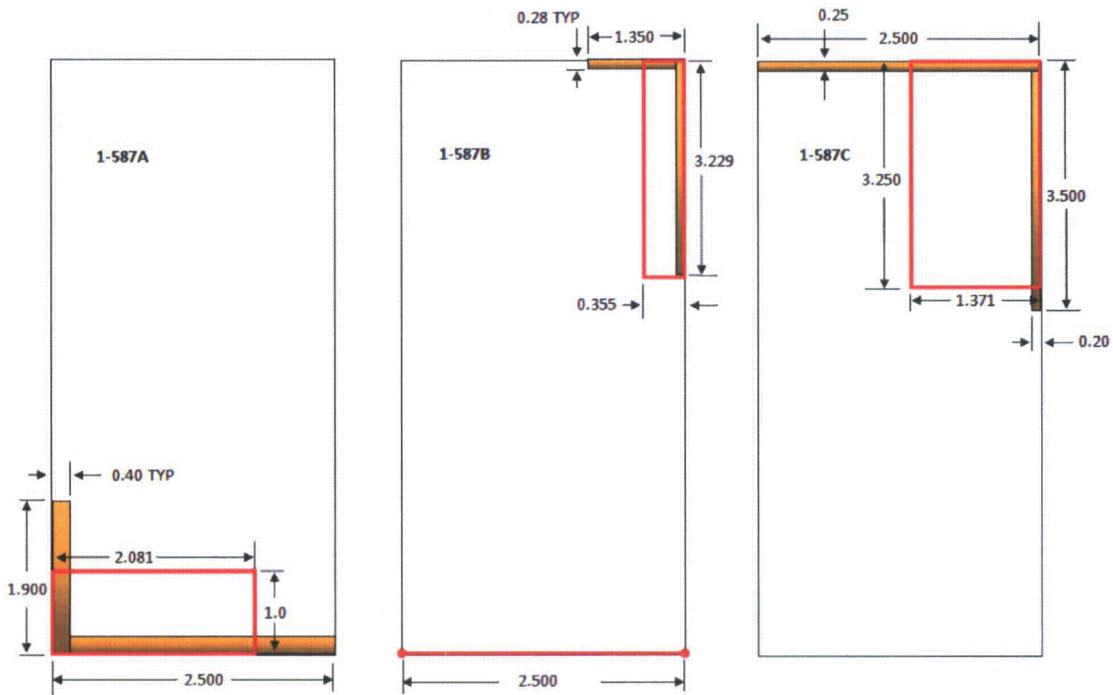


Figure 5. Initial Flaw Characterization (without NDE uncertainty).

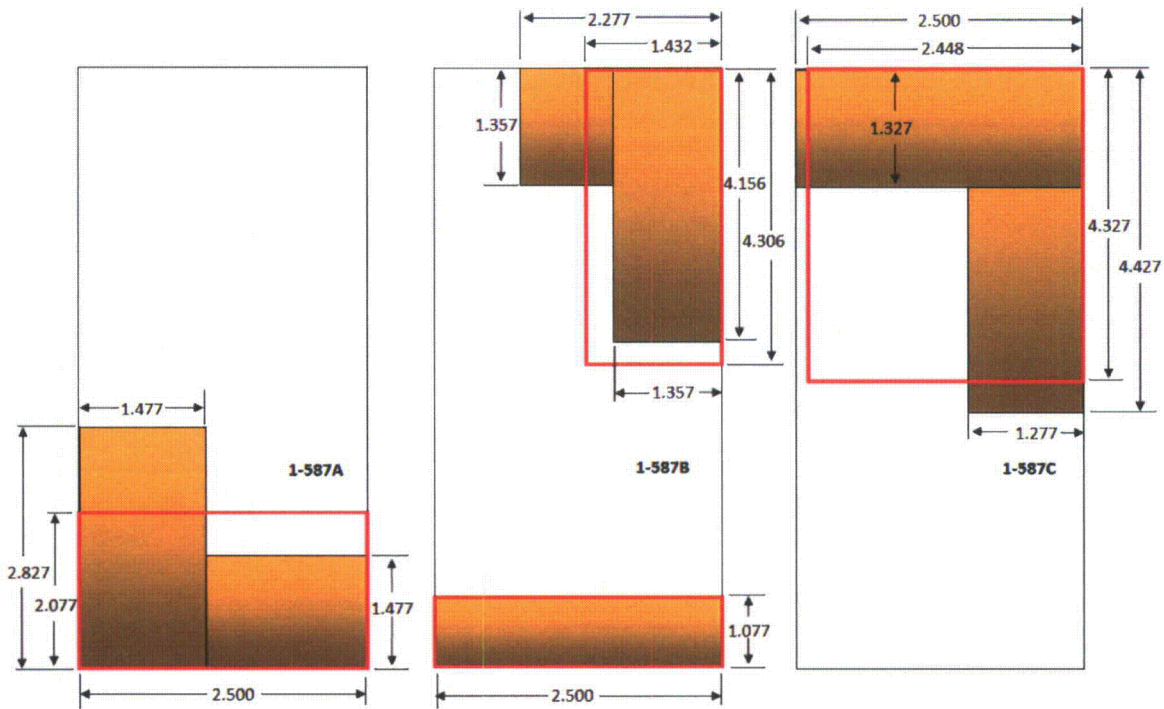


Figure 6. End of Evaluation Interval Flaws (with NDE uncertainty and growth).

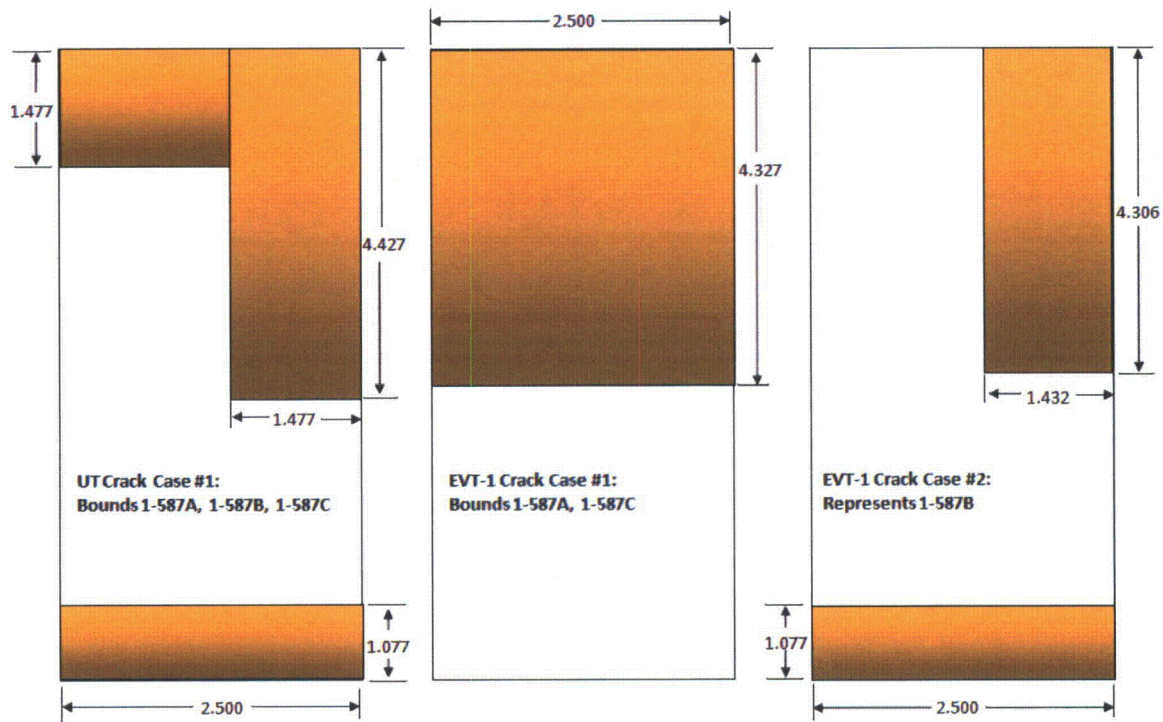


Figure 7. Crack Cases Selected for Flaw Evaluation.

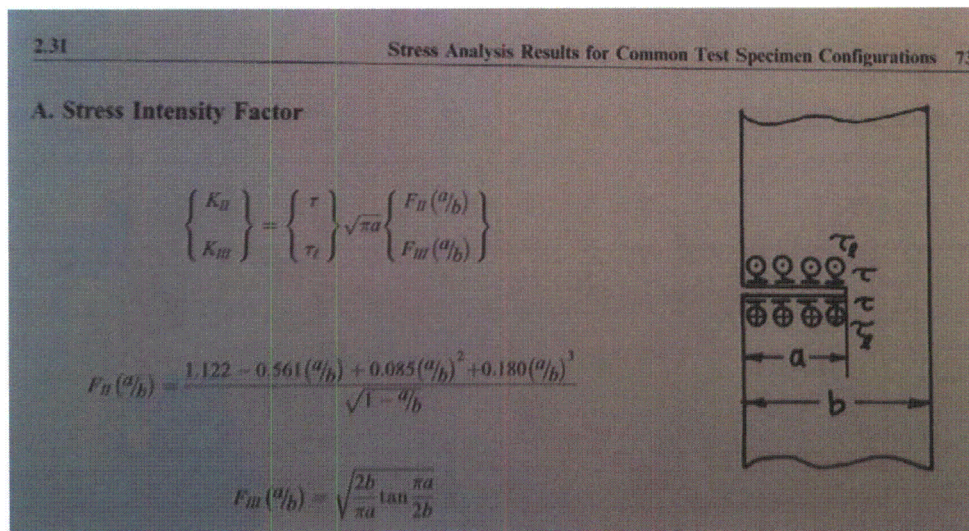
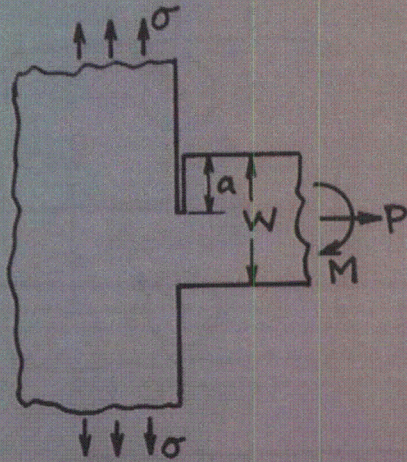


Figure 8. 2-D Edge Cracked Finite Width Plate LFM Solution for In-Plane and Out of Plane Shear [18].



$$A = a/W$$

$$K_I = \sqrt{\pi a} \left[\sigma F_{I\sigma}(A) + \frac{P}{W} F_{IP}(A) + \frac{M}{W^2} F_{IM}(A) \right]$$

$$K_{II} = \sqrt{\pi a} \left[\sigma F_{II\sigma}(A) + \frac{P}{W} F_{IIP}(A) + \frac{M}{W^2} F_{IIM}(A) \right]$$

$$F_{I\sigma}(A) = \sqrt{\frac{1-A}{A}} \cdot \left[0.018 + 0.069 e^{-12.5(\frac{A}{1-A})} \right]$$

$$F_{II\sigma}(A) = \sqrt{\frac{1-A}{A}} \cdot \left[0.156 - 0.067 e^{-8.9(\frac{A}{1-A})} \right]$$

$$F_{IP}(A) = \frac{1}{\sqrt{A(1-A)^{3/2}}} \cdot \left[0.379 + 0.624A - 0.062 e^{-12(\frac{A}{1-A})} \right]$$

$$F_{IIP}(A) = \frac{1}{\sqrt{A(1-A)^{3/2}}} \cdot \left[0.126 - 0.24A - 0.023(1-A)^5 \right]$$

$$F_{IM}(A) = \frac{1}{\sqrt{A(1-A)^{3/2}}} \cdot \left[2.005 - 0.72 e^{-9(\frac{A}{1-A})} \right]$$

$$F_{IIM}(A) = \frac{1}{\sqrt{A(1-A)^{3/2}}} \cdot \left[-0.228 + (1-A)^4 (0.577 - 0.2A + 0.8A^2) \right]$$

Method: Conformal Mapping

Accuracy: F_{IP}, F_{IIP}, F_{IM} 1%; $F_{I\sigma}, F_{II\sigma}, F_{IIM}$ 2%

References: Hasebe 1987; Tada 2000

NOTE: All approximate formulas (Tada 2000) are based on accurate (0.1%) numerical values (Hasebe 1987).

Figure 9. 2-D LEFM Solution Perpendicular Plates Subjected to Axial Force, Bending Moment, and Uniform Membrane Stress in Semi-Infinite Wall [18].

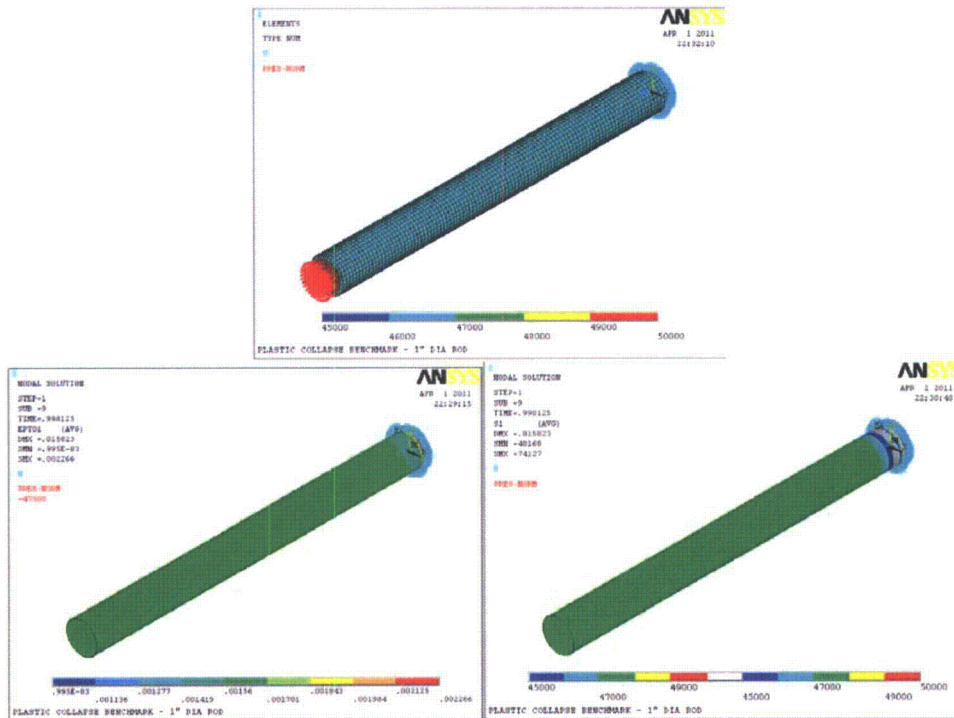


Figure 10. FEM and Results of Plastic Collapse Benchmark.

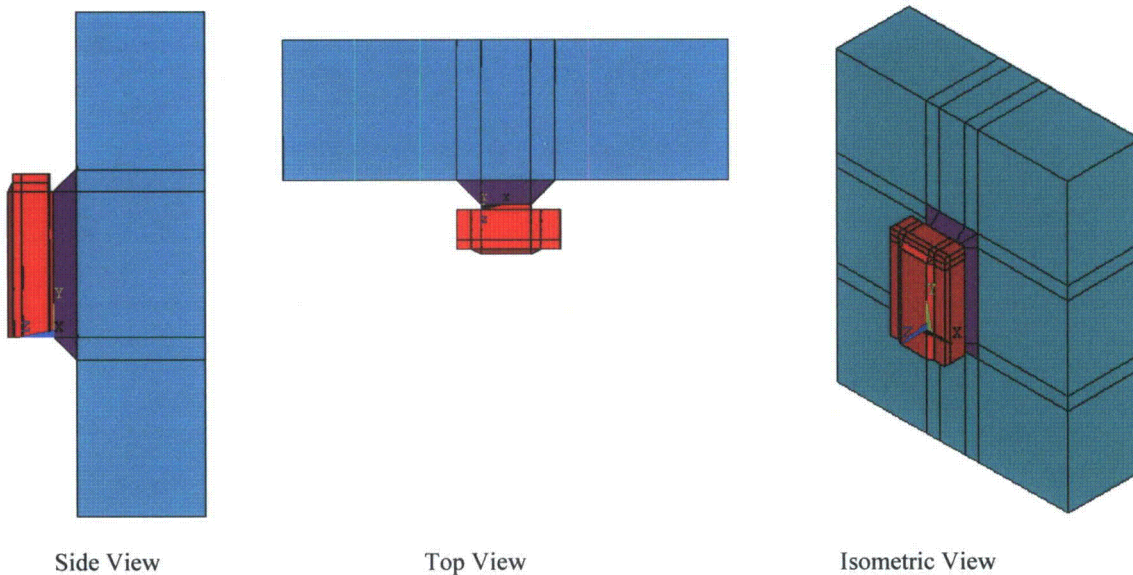


Figure 11. Steam Dryer Support Bracket FEM.

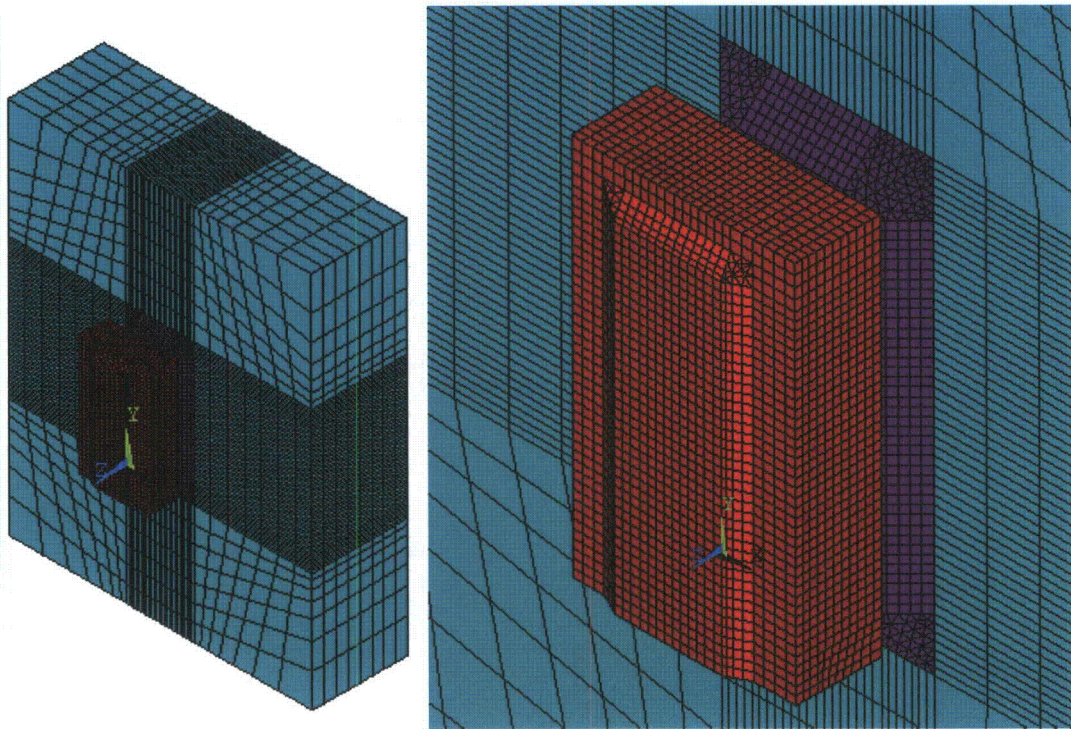


Figure 12. Finite Element Mesh for 0.2 inch Mesh Defined for Support Bracket.

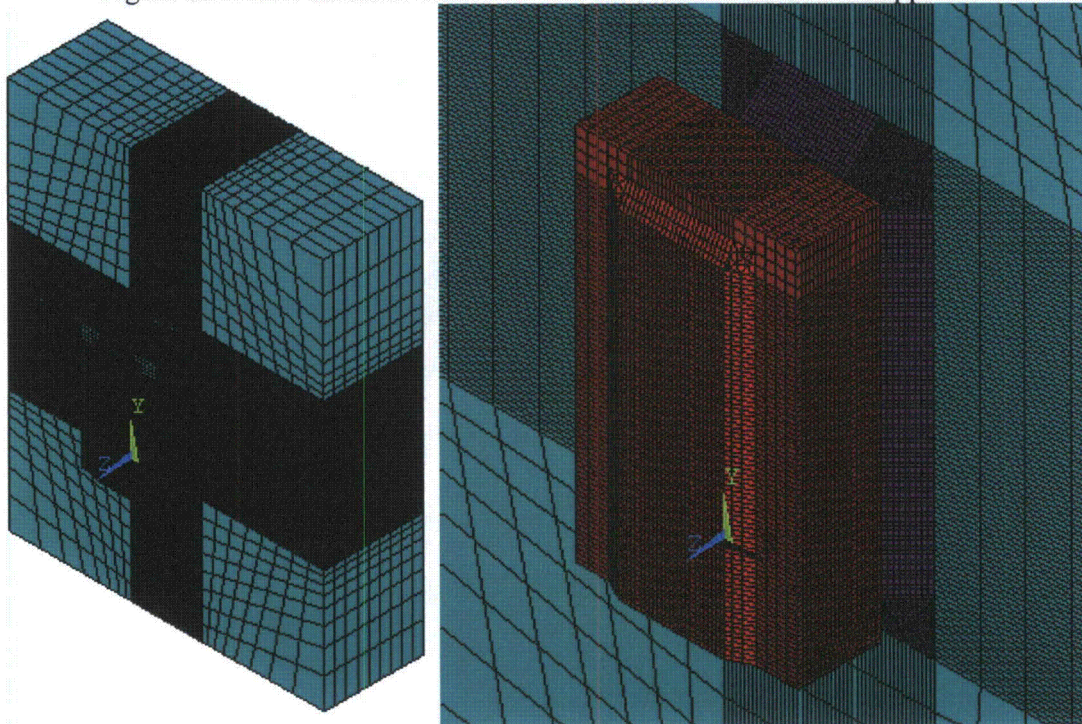


Figure 13. Finite Element Mesh for 0.1 inch Mesh Defined for Support Bracket.

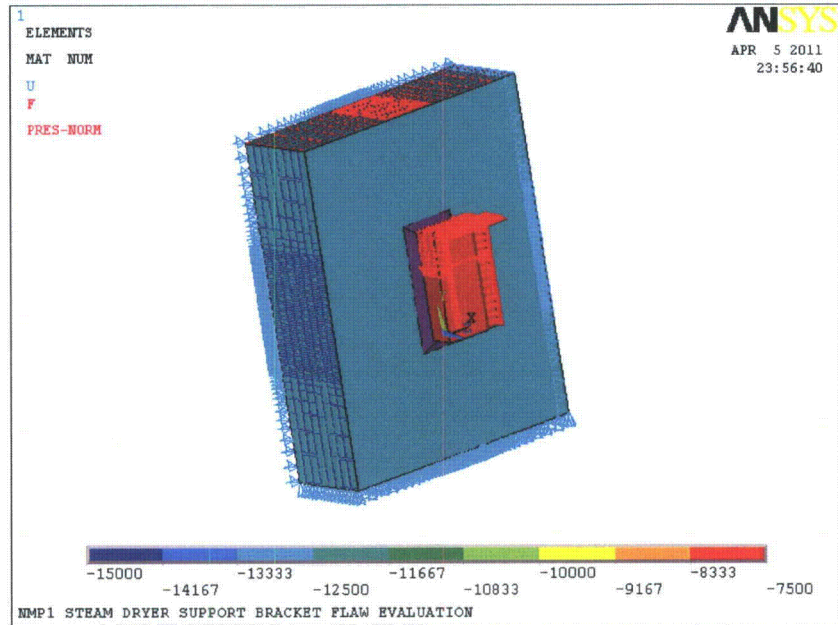


Figure 14. Loads and Boundary Conditions Applied to Support Bracket FEM.

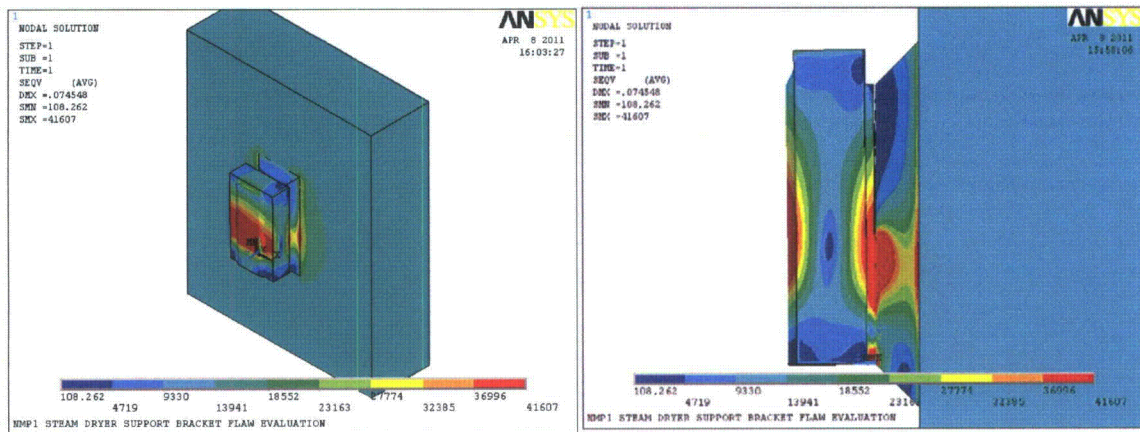
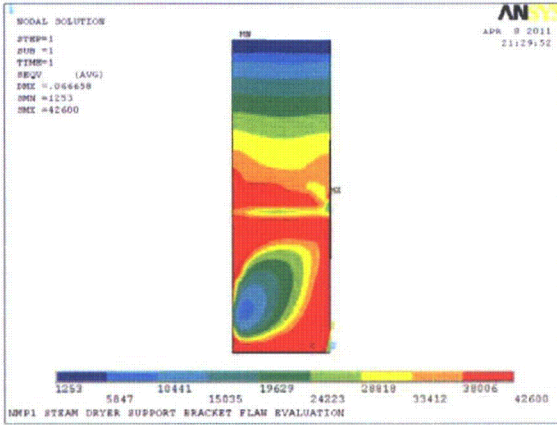
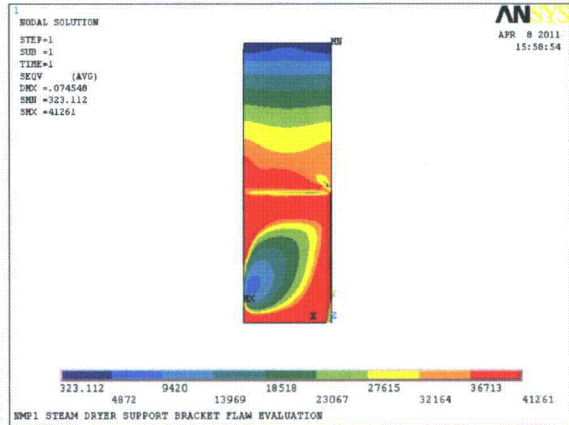


Figure 15. Von Mises Stress for EVT-1 Crack Case 1, 0.1 inch Mesh.

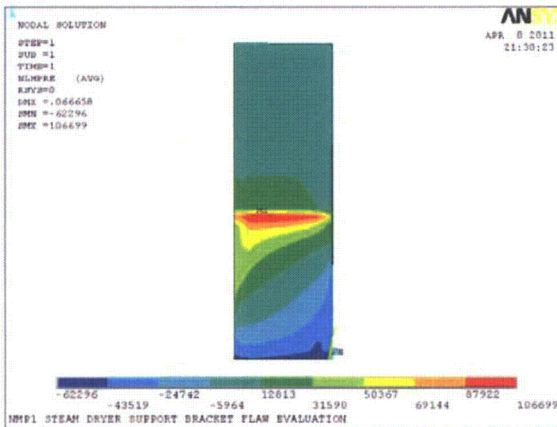


Mesh Size = 0.2 inch

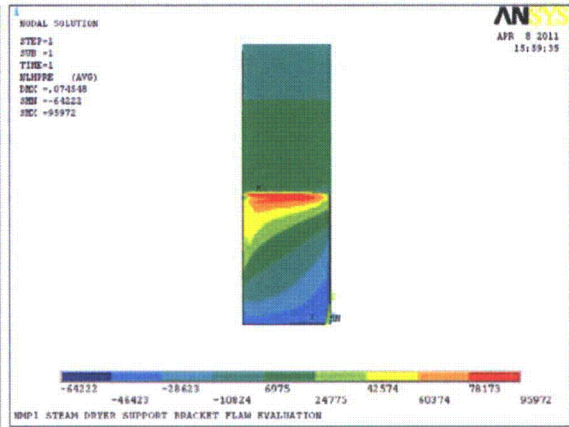


Mesh Size = 0.1 inch

Figure 16. Von Mises Stress on the Crack Plane, EVT-1 Crack Case 1.

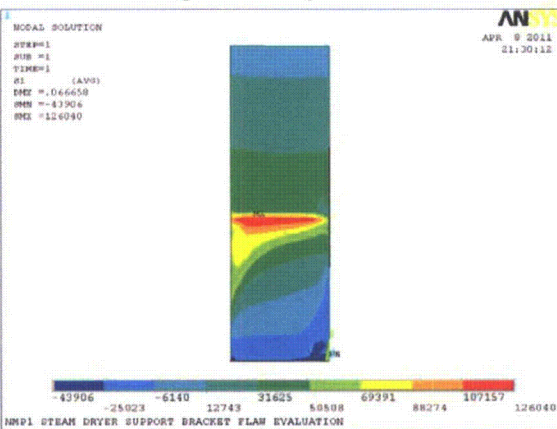


Mesh Size = 0.2 inch

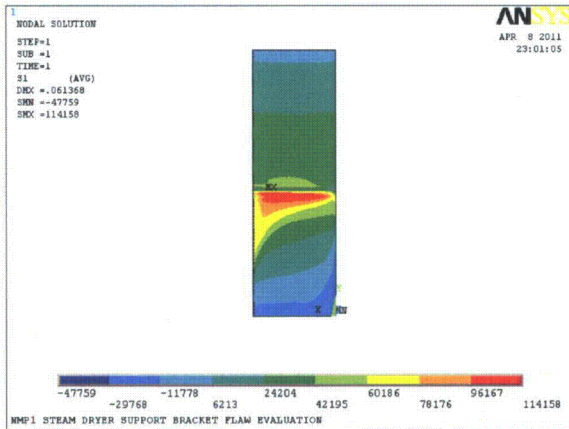


Mesh Size = 0.1 inch

Figure 17. Hydrostatic Stress on the Crack Plane, EVT-1 Crack Case 1.



Mesh Size = 0.2 inch



Mesh Size = 0.1 inch

Figure 18. Maximum Principal Stress on the Crack Plane, EVT-1 Crack Case 1.

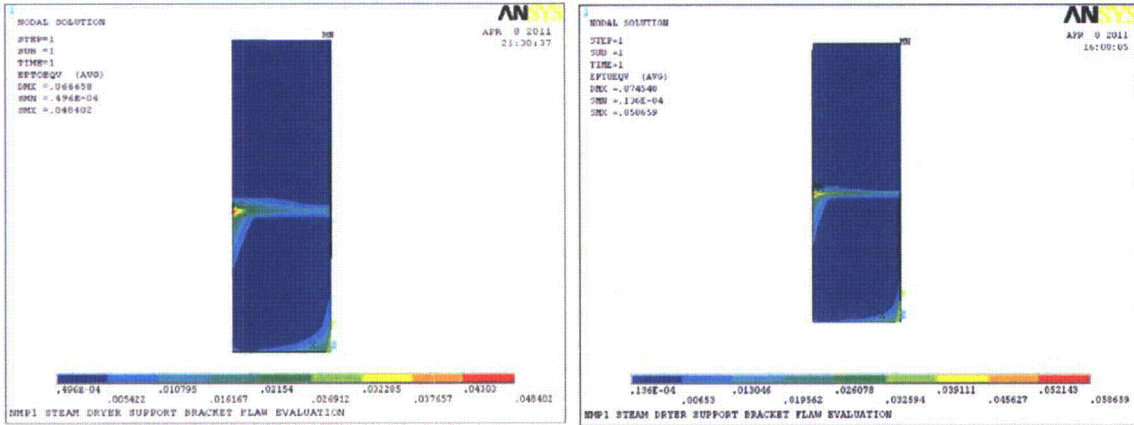


Figure 19. Von Mises Strain on the Crack Plane, EVT-1 Crack Case 1.

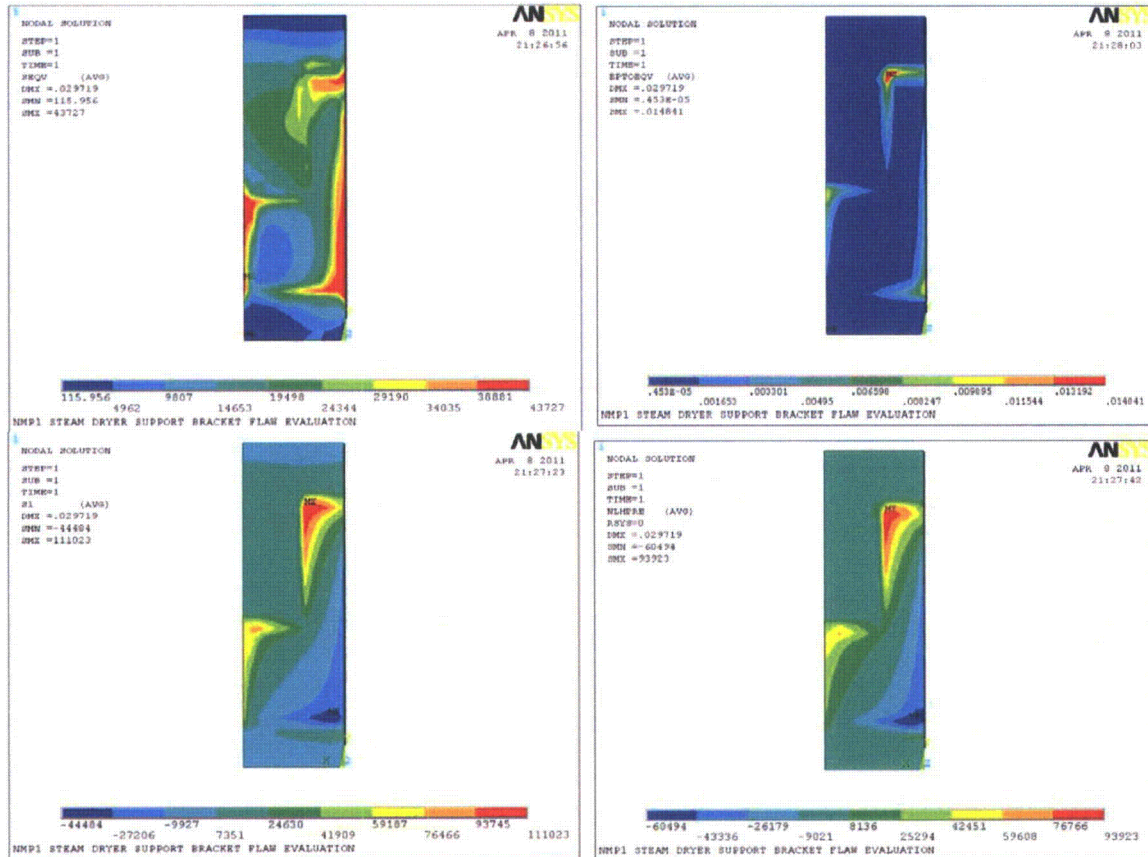


Figure 20. Von Mises Stress (top left), Von Mises Strain (top right), Maximum Principal Stress (bottom left), and Hydrostatic Stress (bottom right) on the Crack Plane, Crack Case UT-1.

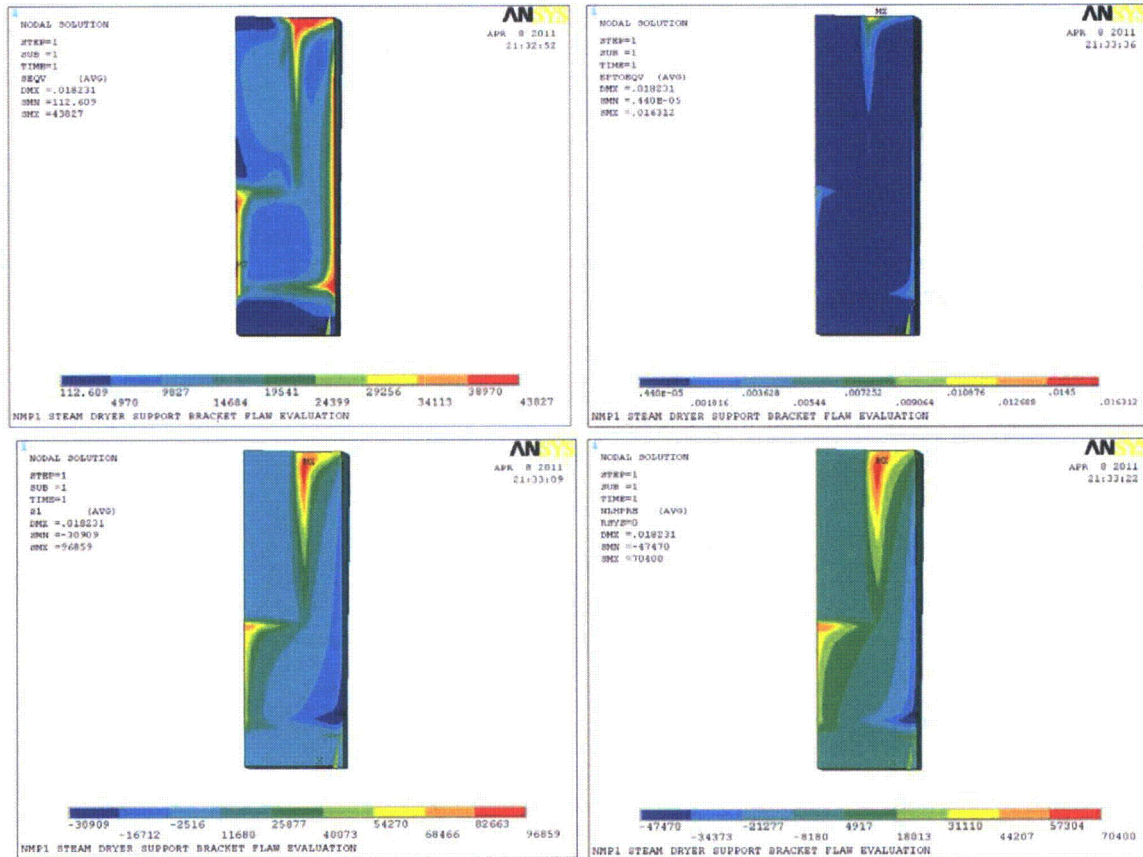
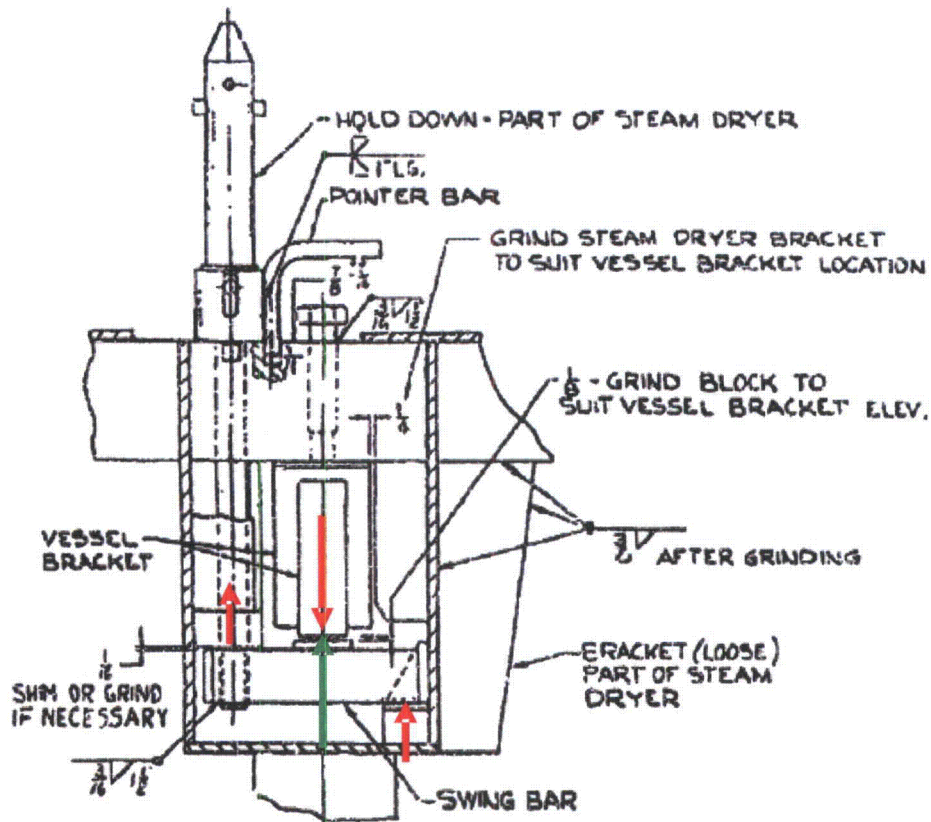


Figure 21. Von Mises Stress (top left), Von Mises Strain (top right), Maximum Principal Stress (bottom left), and Hydrostatic Stress (bottom right) on the Crack Plane, Crack Case EVT-2.



HOLD DOWN IN LOCKED POSITION

- Notes: 1. Arrows indicate forces acting on swing bar (**RED**) and vessel bracket (**GREEN**).
 2. Length of arrow indicates an approximate, relative, magnitude of the force.

Figure 22. Steam Dryer Hold-down Assembly Configuration.



Figure 23. Photograph of Steam Dryer Hold-down Assembly in Open Configuration (Not Installed on Support Bracket).

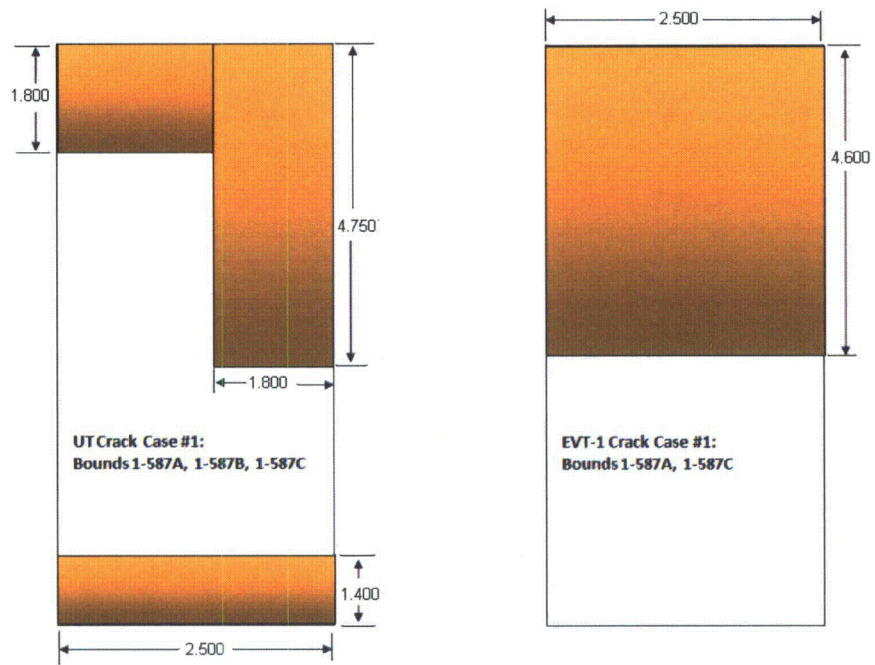
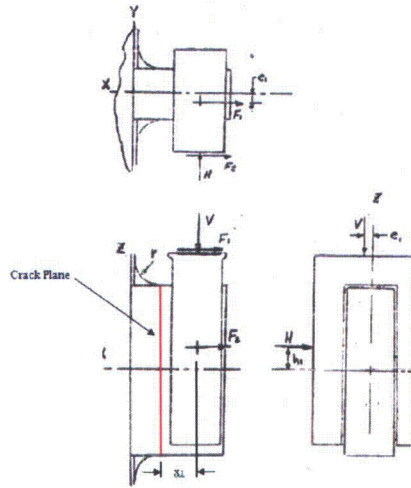


Figure 24. End of Interval Allowable Flaw Sizes.

APPENDIX A
LEFM ANALYSIS



Note: $e_1 = 0.25$ inches
 $h_1 = 1.0$ inches
 $x_1 = 1.25$ inches

For the configuration shown above the stress intensity factor at the crack plane is determined by superposition of the following LEFM solutions found in The Stress Analysis of Cracks:

1. Edge cracked finite width plate subjected to in plane and out of plane shear stresses (pg. 73)
2. Semi-infinite 90 degree plate intersection with edge crack at intersection subjected to axial force, moment, and membrane stress (pg. 307).

From pg. 73:

$$KII = \tau \sqrt{\pi a} \cdot FII$$

$$FII = \frac{1.122 - 0.561 \left(\frac{a}{b}\right) + 0.085 \left(\frac{a}{b}\right)^2 + 0.180 \left(\frac{a}{b}\right)^3}{\sqrt{1 - \frac{a}{b}}}$$

$$KIII = \tau_1 \sqrt{\pi a} \cdot FIII$$

$$FIII = \sqrt{\frac{2b}{\pi a} \cdot \tan\left(\frac{\pi a}{2b}\right)}$$

$$KI = \sqrt{\pi a} \cdot \left(\sigma \cdot FI\sigma(A) + \frac{P}{W} \cdot FIp(A) + \frac{M}{W^2} \cdot FIIm(A) \right)$$

$$KII = \sqrt{\pi a} \cdot \left(\sigma \cdot FII\sigma(A) + \frac{P}{W} \cdot FIIp(A) + \frac{M}{W^2} \cdot FIIIm(A) \right)$$

$$A(a, W) = \frac{a}{W}$$

$$FI\sigma(A) = \sqrt{\frac{1-A}{A}} \cdot \left[0.018 + 0.069e^{-12.5 \cdot \left(\frac{A}{1-A}\right)} \right]$$

$$FII\sigma(A) = \sqrt{\frac{1-A}{A}} \cdot \left[0.156 - 0.067e^{-8.9 \cdot \left(\frac{A}{1-A}\right)} \right]$$

$$FIp(A) = \frac{1}{\sqrt{A} \cdot (1-A)^{\frac{3}{2}}} \cdot \left[0.379 + 0.624A - 0.062e^{-12 \cdot \left(\frac{A}{1-A}\right)} \right]$$

$$FIIp(A) = \frac{1}{\sqrt{A} \cdot (1-A)^{\frac{3}{2}}} \cdot \left[0.126 - 0.24A - 0.023(1-A)^5 \right]$$

$$FIIm(A) = \frac{1}{\sqrt{A} \cdot (1-A)^{\frac{3}{2}}} \cdot \left[2.005 - 0.72e^{-9 \cdot \left(\frac{A}{1-A}\right)} \right]$$

$$FIIIm(A) = \frac{1}{\sqrt{A} \cdot (1-A)^{\frac{3}{2}}} \cdot \left[-0.228 + (1-A)^4 \cdot (0.577 - 0.2A + 0.8A^2) \right]$$

For Axial stress orientation (i.e. longitudinal axis of RPV)

$$a := 4.45 \text{ in}$$

$$W := 8 \text{ in}$$

$$b := W$$

$$A := \frac{a}{W} \quad A = 0.556$$

$$\tau := \frac{18750}{2.5 \cdot 8} \quad \tau = 937.5$$

$$\tau_l := \frac{(162501 - 18.75 \cdot 0.25) \cdot (1.25^2 + 4^2)^{0.5}}{\frac{1}{12} \cdot (8 \cdot 1.25^3 + 2.5 \cdot 4^3)} \quad \tau_l = 4652$$

$$F_{II} := \frac{1.122 - 0.561 \left(\frac{a}{b}\right) + 0.085 \left(\frac{a}{b}\right)^2 + 0.180 \left(\frac{a}{b}\right)^3}{\sqrt{1 - \frac{a}{b}}} \quad F_{II} = 1.302$$

$$K_{II_1} := \tau \cdot \sqrt{\pi \cdot a} \cdot F_{II} \quad K_{II_1} = 4563$$

$$F_{III} := \sqrt{\frac{2 \cdot b}{\pi \cdot a} \cdot \tan\left(\frac{\pi \cdot a}{2 \cdot b}\right)} \quad F_{III} = 1.169$$

$$K_{III} := \tau_l \cdot \sqrt{\pi \cdot a} \cdot F_{III} \quad K_{III} = 20335$$

$$\sigma := \frac{1000 \cdot \frac{213.44}{2}}{2 \cdot 7.125} \quad \sigma = 14978 \quad \text{psi}$$

$$P := \frac{20000}{W} \quad P = 8000 \quad \frac{\text{lb}}{\text{in}}$$

$$M := \frac{150005 + 187501.25 + 50001}{W} \quad M = 14625 \quad \frac{\text{lb}}{\text{in}^2}$$

$$FI\sigma := \sqrt{\frac{1-A}{A}} \cdot \left[0.018 + 0.069e^{-12.5 \cdot \left(\frac{A}{1-A}\right)} \right]$$

FI σ = 0.016

$$FII\sigma := \sqrt{\frac{1-A}{A}} \cdot \left[0.156 - 0.067e^{-8.9 \cdot \left(\frac{A}{1-A}\right)} \right]$$

FII σ = 0.139

$$FIp := \frac{1}{\sqrt{A} \cdot (1-A)^{\frac{3}{2}}} \cdot \left[0.379 + 0.624A - 0.062e^{-12 \cdot \left(\frac{A}{1-A}\right)} \right]$$

FIp = 3.293

$$FIIp := \frac{1}{\sqrt{A} \cdot (1-A)^{\frac{3}{2}}} \cdot \left[0.126 - 0.24A - 0.023(1-A)^5 \right]$$

FIIp = -0.036

$$FIIm := \frac{1}{\sqrt{A} \cdot (1-A)^{\frac{3}{2}}} \cdot \left[2.005 - 0.72e^{-9 \cdot \left(\frac{A}{1-A}\right)} \right]$$

FIIm = 9.094

$$FIIIm := \frac{1}{\sqrt{A} \cdot (1-A)^{\frac{3}{2}}} \cdot \left[-0.228 + (1-A)^4 \cdot (0.577 - 0.2A + 0.8A^2) \right]$$

FIIIm = -0.909

$$KI := \sqrt{\pi \cdot a} \cdot \left(\sigma \cdot FI\sigma + \frac{P}{W} \cdot FIp + \frac{M}{W^2} \cdot FIIm \right)$$

KI = 11168 psi· $\sqrt{\text{in}}$

$$KII_2 := \sqrt{\pi \cdot a} \cdot \left(\sigma \cdot FII\sigma + \frac{P}{W} \cdot FIIp + \frac{M}{W^2} \cdot FIIIm \right)$$

KII_2 = 3173 psi· $\sqrt{\text{in}}$

An equivalent KI may be given by:

$$\nu = 0.3$$

$$KI_{eq} := \left[KI^2 + (KII_1 + KII_2)^2 + \frac{1}{1-\nu} \cdot KIII^2 \right]^{0.5}$$

KI_{eq} = 27845 psi· $\sqrt{\text{in}}$

The static fracture toughness for unirradiated stainless steel is taken from BWRVIP-76 as 150 ksi-in^{0.5}. The required structural factor for Level A/B conditions is taken as 2.7. Therefore, the allowable fracture toughness for stainless steel is given as:

$$KI_{\text{allowable}} := \frac{150}{2.7} \quad KI_{\text{allowable}} = 55.6 \quad \text{ksi} \cdot \text{in}^{0.5}$$

Considering a flaw oriented on either axis of the support bracket the applied stress intensity factor is less than the allowable fracture toughness.

Calculation of Plastic Zone Correction

$$KI_{\text{eq}} = 27845 \quad \text{psi} \cdot \text{in}^{0.5}$$

$$\sigma_y = 18300 \quad \text{psi}$$

$$r_Y := (KI_{\text{eq}} / \sigma_y)^2 / 6\pi$$

$$r_Y = 0.123 \text{ in.}$$

ATTACHMENT 3

**AFFIDAVIT
FROM EPRI JUSTIFYING WITHHOLDING PROPRIETARY
INFORMATION**

July 14, 2011

Document Control Desk
Office of Nuclear Reactor Regulation
U.S. Nuclear Regulatory Commission
Washington, DC 20555-0001

Attention: Jonathan Rowley

Subject: Request for Withholding of the following Proprietary Information Included in:

“Nine Mile Point Unit 1: Steam Dryer Support Bracket Flaw Evaluation”
Structural Integrity Associates Report No. 1100539.401
Revision 1, Project No. 1100539, July 2011

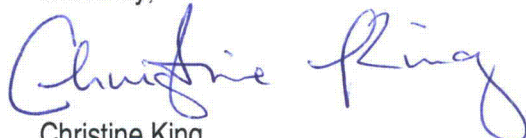
To Whom It May Concern:

This is a request under 10 C.F.R. §2.390(a)(4) that the U.S. Nuclear Regulatory Commission (“NRC”) withhold from public disclosure the report identified in the enclosed Affidavit consisting of the proprietary information (“the Proprietary Information”) owned by Electric Power Research Institute, Inc. (“EPRI”) identified in the attached report. Proprietary and non-proprietary versions of the report, which contain the Proprietary Information, and the Affidavit in support of this request are enclosed.

EPRI desires to disclose the information in confidence for informational purposes regarding a submittal to the NRC by Constellation Energy. The Proprietary Information is not to be divulged to anyone outside of the NRC or to any of its contractors, nor shall any copies be made of the Information provided herein. EPRI welcomes any discussions and/or questions relating to the information enclosed.

If you have any questions about the legal aspects of this request for withholding, please do not hesitate to contact me at (650) 855-2164. Questions on the content of the correspondence should be directed to Randy Stark of EPRI at (650) 855-2122.

Sincerely,



Christine King
Sr. Manager, Business & Operations

c: Sheldon Stuchell, NRC (Sheldon.stuchell@nrc.gov)

AFFIDAVIT

RE: Request for Withholding of the Following Proprietary Information Included in:

“Nine Mile Point Unit 1: Steam Dryer Support Bracket Flaw Evaluation”
Structural Integrity Associates Report No. 1100539.401
Revision 1, Project No. 1100539, July 2011

I, Christine King, being duly sworn, depose and state as follows:

I am the Senior Manager of Business & Operations in the Nuclear Power Sector at Electric Power Research Institute, Inc. whose principal office is located at 3420 Hillview Avenue, Palo Alto, California (“EPRI”) and I have been specifically delegated responsibility for the above-listed document that contains EPRI proprietary information that is sought under this Affidavit to be withheld (“Proprietary Information”). I am authorized to apply to the U.S. Nuclear Regulatory Commission (“NRC”) for the withholding of the Proprietary Information on behalf of EPRI.

EPRI requests that the Proprietary Information be withheld from the public on the following bases:

Withholding Based Upon Privileged And Confidential Trade Secrets Or Commercial Or Financial Information:

a. The Proprietary Information is owned by EPRI and has been held in confidence by EPRI. All entities accepting copies of the Proprietary Information do so subject to written agreements imposing an obligation upon the recipient to maintain the confidentiality of the Proprietary Information. The Proprietary Information is disclosed only to parties who agree, in writing, to preserve the confidentiality thereof.

b. EPRI considers the Proprietary Information contained therein to constitute trade secrets of EPRI. As such, EPRI holds the information in confidence and disclosure thereof is strictly limited to individuals and entities who have agreed, in writing, to maintain the confidentiality of the Information. EPRI made a substantial economic investment to develop the Proprietary Information contained in the report and, by prohibiting public disclosure, EPRI derives an economic benefit in the form of licensing royalties and other additional fees from the confidential nature of the Proprietary Information. If the Proprietary Information were publicly available to consultants and/or other businesses providing services in the electric and/or nuclear power industry, they would be able to use the Proprietary Information for their own commercial benefit and profit and without expending the substantial economic resources required of EPRI to develop the Proprietary Information.

c. EPRI’s classification of the Proprietary Information as trade secrets is justified by the Uniform Trade Secrets Act which California adopted in 1984 and a version of which has been adopted by over forty states. The California Uniform Trade Secrets Act, California Civil Code §§3426 – 3426.11, defines a “trade secret” as follows:

"Trade secret" means information, including a formula, pattern, compilation, program device, method, technique, or process, that:

(1) Derives independent economic value, actual or potential, from not being generally known to the public or to other persons who can obtain economic value from its disclosure or use; and

(2) Is the subject of efforts that are reasonable under the circumstances to maintain its secrecy."

d. The Proprietary Information contained therein is not generally known or available to the public. EPRI developed the Information only after making a determination that the Proprietary Information was not available from public sources. EPRI made a substantial investment of both money and employee hours in the development of the Proprietary Information. EPRI was required to devote these resources and effort to derive the Proprietary Information. As a result of such effort and cost, both in terms of dollars spent and dedicated employee time, the Proprietary Information is highly valuable to EPRI.

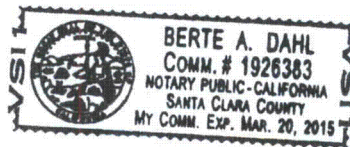
e. A public disclosure of the Proprietary Information would be highly likely to cause substantial harm to EPRI's competitive position and the ability of EPRI to license the Proprietary Information both domestically and internationally. The Proprietary Information can only be acquired and/or duplicated by others using an equivalent investment of time and effort.

I have read the foregoing and the matters stated herein are true and correct to the best of my knowledge, information and belief. I make this affidavit under penalty of perjury under the laws of the United States of America and under the laws of the State of California.

Executed at 3420 Hillview Avenue, Palo Alto, CA 94304-1395 being the premises and place of business of Electric Power Research Institute, Inc.

Date: July 14, 2011

Christine King
Christine King



(State of California)
(County of Santa Clara)

Subscribed and sworn to (or affirmed) before me on this 14th day of July, 2011, by _____, proved to me on the basis of satisfactory evidence to be the person(s) who appeared before me.

Signature Berthe A. Dahl (Seal)

My Commission Expires 20 day of March, 2014.